

Seismic Architecture of the Archean North American Mantle
and its Relation to Diamondiferous Kimberlite Fields

**STÉPHANE FAURE¹, STÉPHANIE GODEY², FRANCINE FALLARA³ AND SYLVAIN
TRÉPANIÉ¹**

1- CONSOREM Consortium de Recherche en Exploration Minérale, Université du Québec à Montréal, Montréal (Québec), Canada, H3C 3P8 faure.stephane@uqam.ca

2- EMSC/CSEM European Mediterranean Seismological Centre, Bruyères le Châtel 91680, France

3- URSTM Unité de Recherche et de Service en Technologie Minérale, Université du Québec en Abitibi-Témiscamingue, Rouyn-Noranda (Québec), Canada, J9X 5E4

Published in Economic Geology, v. 106, pp. 223–240 (2011)

Abstract

The seismic architecture of the average Archean-only mantle beneath exposed and sub-surface Archean crust of the U.S. and Canada is presented here in three dimensions (3D) for the first time using a high lateral resolution Rayleigh wave phase velocity model of the upper mantle (30-250 km depth). The morphology of the cratonic coherent mantle is compared with other regional and local geophysical models, geologic interpretations, and published xenolith barometric studies. In particular, the kimberlite magma source regions at the Lithosphere-Asthenosphere Boundary inferred from xenolith data are consistent with the bottom topography of the Archean seismic mantle signature. The characteristic fast seismic response found beneath much of the exposed Archean crust is also found in Canada beneath some covered terranes, sedimentary basins, and Proterozoic mobile belts.

The northeastern and northwestern parts of the Superior craton host, with the central Hearne craton, the deepest mantle roots of North America (225 to 240 km depth). However, the southern portion of the Superior craton is characterized by an east-west channel that is 30 percent slower in seismic velocity than its northern counterpart. This contrasting seismic signature correlates with the location of the southernmost Neoproterozoic greenstone belts and to their plume-driven subduction zones. The scar in the mantle produced by this early tectonothermal event has been reused by widespread and sporadic carbonatite and kimberlite magmatic events spanning from the Early Proterozoic to the Cretaceous, and as a consequence, the diamond stability field has been partially to totally overprinted.

Almost all diamondiferous kimberlites in Canada are located vertically over an interval of 160 to 200 km depth in areas of steep slopes surrounding deep (180 to 240 km), relatively small, and flat-bottomed Paleo-Mesoarchean cratonic keels.

Introduction

The diamond potential of kimberlites depends first and foremost on favorable pressure and temperature conditions preserved at depths greater than 150 km in the underlying sub-continental mantle lithosphere (Boyd et al., 1985). Since the first global seismic tomography, geologists have known that velocity anomalies correlate well with the age of surface materials and that seismically fast velocity anomalies correspond to Precambrian, relatively cold, and predominantly depleted peridotitic upper mantle (Anderson et al., 1992; Polet and Anderson, 1995; van der Lee, 2001). These tectonically stable areas are particularly sought-after, because most gem-diamond bearing kimberlites originate from Archean cratonic mantle roots and, for instance, form the only viable economic deposits worldwide (Gurney et al., 2005). Although the surface exposure of the Archean crust is well documented, the extent of the underlying mantle keel is not well constrained. Understanding the 3D mantle architecture of ancient mantle roots, where diamond reservoirs have survived all igneous and tectonic processes since the Archean, thus provides important clues for regional-scale exploration of diamondiferous kimberlites.

In North America, the composition and major boundaries of cratonic keels are partially constrained by xenolith studies of some 40 kimberlites or other mantle-related magmatic fields (Griffin et al., 2004 among others). Several seismic transects have imaged the crust and uppermost part of the mantle in 2D, mostly at cratonic margins and at an investigation depth of less than 80 km (Lithoprobe projects; Clowes et al., 1992). However, the geometry of the diamond-fertile sub-continental mantle is poorly constrained and an estimation of its volume has never been proposed. The recognition of the long-term storage and preservation of diamonds in cratonic roots is fundamental to evaluating the global budget of the resource.

Attempts to define the 3D Archean mantle architecture are of prime importance since only 25 percent of worldwide kimberlites and lamproites are located in exposed Archean rocks. Most remaining kimberlites occur underneath younger sedimentary basins and platforms. From the present day distribution of kimberlite fields, two major questions can be asked. Firstly, why do kimberlites occur only in certain parts of Archean cratons, and secondly, are there other kimberlite fields that can be found elsewhere, perhaps off-craton, underneath sedimentary cover?

In this paper, we address the problem of diamondiferous kimberlite distribution relative to the seismic signature of the depleted Archean mantle roots. For this, we present a high lateral resolution Rayleigh wave phase velocity model that covers both Canada and the United States. The tomographic model is compared with both the exposed and covered (or sub-surface) Archean crust. The morphology of the seismic Archean upper mantle is presented in 3D and its spatial relationship with known kimberlite fields and inferred magma sources at depth, estimated from published xenolith studies, is discussed. Finally, a new geological model that explains the distribution of diamondiferous kimberlites relative to the Mesoproterozoic cratonic nuclei is proposed.

S-Wave 3D Tomographic Model

Seismic tomography is a deep-sounding geophysical method capable of depicting the present-day 3D image of seismic anomalies in the mantle. By calculating the relative travel time of seismic waves from source to receiver for example, and inverting them for subcrustal velocity anomalies, seismic tomography reveals heterogeneities in mantle velocity which are directly related to the temperature and composition of the mantle (Forte and Perry, 2000).

Higher than average velocities indicate the presence of stable iron-depleted, colder mantle compared to the global average.

Previous Work

Many tomographic models beneath North America have been proposed. They focus on different length scales (local to regional) and use types of data varying from body waves and surface waves to full waveforms. Grand (1994) presented a large scale S-velocity model of the Americas using body waves. Alsina et al. (1996) and van der Lee and Nolet (1997) proposed S-wave velocity models for the continental United States and imaged portions of the Precambrian cratonic root and adjacent mantle below the U.S. Frederiksen et al. (2001) presented a surface wave model for Canada only, whereas Levshin et al. (2001) covered the entire Arctic above 60°N latitude. More recently, continental-scale models have been published for the entire North America (Godey et al., 2003; van der Lee and Frederiksen, 2005; Nettles and Dziewoński, 2008; Bedle and van der Lee, 2009; Yuan and Romanowicz, 2010). In addition, several local body and surface wave studies were performed throughout the continent, particularly in the tectonic southwest, but also in Canada's Northwest Territories (Bank et al., 1998) and Superior Province (Rondenay et al., 2000; Sol et al., 2002; Darbyshire et al., 2007; Frederiksen et al., 2007).

The shear wave velocity model used in this study is a high-resolution model covering Canada and the U.S., published by Godey et al. (2003). The main contribution of this robust model was to close the gap between local and global tomography studies and provide a better surface wave phase velocity map with an improved lateral resolution across North America.

Data and Methodology

The shear wave velocity model is derived from a dataset of 207 seismic events. The events occurred in North America and the Caribbean between 1995 and 1999 with a magnitude range of 4.9 to 7.0 and were recorded by global and regional networks (Godey et al., 2003). Phase velocity maps were first constructed for the period range 40 to 150s using 7,700 Rayleigh wave fundamental mode phase velocity dispersion curves selected by the automatic waveform inversion of Trampert and Woodhouse (1995), allowing a homogeneous coverage at all periods. Secondly, the phase velocity measurements corrected for crustal structure using the model CRUST5.1 (Mooney et al., 1998) were inverted to obtain phase velocity maps. Velocities are described as percentage variations to the Preliminary Reference Earth Model (PREM; Dziewonski and Anderson, 1981). Rayleigh wave phase velocities at a given geographic point are primarily sensitive to the local depth profile of the S and P waves. Assuming a constant ratio between shear and compressional velocities (Robertson and Woodhouse, 1997), we can infer S velocity structure at depth from the phase velocity maps (see Godey 2002 for details). Using our period range, we can resolve shear wave velocity structure between 50 and 250 km depth. The S velocity model is obtained by standard least squares inversion for spline functions using a model regularization function.

Spatial resolution and the accuracy of the model depend on the data coverage and the depth considered. The difference between the observed and predicted phase velocity dispersion curves and maps does not exceed 1%, indicating that our model is robust and that geologic features are well resolved. On average, a lateral resolution of 800 km is obtained for the whole region with a maximum between 200 and 400 km in the western United States and southern Canada. However, the model reaches better resolution than the local average in a window at

around 150 km, the principal region of interest for our purpose. Below 250 km depth, the resolution is less reliable for imaging of velocity heterogeneities. Average vertical resolution is estimated to be about 50 km. This range of resolution can be viewed as indicative because the direct conversion from mathematical resolution of the model to dimension of geologic features is not straightforward. It is not because a geological feature in an area has a dimension smaller than the resolution of the model that the object cannot be observed; features of smaller scales are retrieved, though their dimension or amplitude can be biased. However velocity anomalies with a spatial dimension of 400 km are very well resolved.

The 3D model is expressed as a percentage velocity perturbation relative to PREM. As an example, 0 represents a velocity equal to that of PREM and +5 percent represents anomalies that are 5 percent faster than the average. S-wave velocity perturbation maps were constructed at intervals of 5 km depth and extrapolated in a 3D space block model within the Gocad© technology environment.

Archean Subcratonic Mantle Seismic Signatures beneath North America

Almost all global and regional tomographic models have compared the velocity structures of the mantle beneath Precambrian shields without differentiating the Archean and the Proterozoic components (Polet and Anderson, 1995; van der Lee and Nolet, 1997; Frederiksen et al., 2001; van der Lee, 2002). However, there is a fundamental difference in the composition, density, thickness, and seismic response between these two components (Durrheim and Mooney, 1994; Artemieva and Mooney, 2001; O'Reilly et al., 2001; Petitjean et al., 2006; Arndt et al., 2009; Artemieva, 2009). The subcratonic Archean mantle is often thicker (200 to 350 km) and is thought to involve lithospheric formation above high-temperature melting

conditions by mantle plumes and buoyant shallow subduction (Artemieva and Mooney, 2002; Foley et al., 2003). The higher temperature of the Archean mantle produces a refractory lithospheric mantle which is ultra-depleted in FeO, Al, Ti, Ca and volatiles (Boyd, 1989; Griffin et al., 2003). Consequently, the resultant lithospheric keel has negative thermal buoyancy compared to the surrounding mantle and also has a high degree of rigidity due to its anhydrous composition. It is not generally susceptible to delamination, and may survive several orogenies and thermomechanical erosion (Durrheim and Mooney, 1994; Afonso and Ranalli, 2004; Petitjean et al., 2006). The Proterozoic mantle consists of strongly reworked (refertilized) Archean lithospheric mantle (Griffin et al., 2009), has an intermediate thickness (100-260 km) and is slightly denser, less conductive and seismically slower (O'Reilly et al., 2001; Artemieva and Mooney, 2002).

The next three sections will present the mantle seismic characteristics beneath exposed and sub-surface Archean crust of the North American Archean cratons.

Upper Mantle Seismic Signatures Under Exposed Archean Crust

In Canada and the U.S., the vertical correspondence between exposed Archean rocks and high seismic velocity structures is obvious, except for the Wyoming and the southern Superior cratons (Fig. 1). The seismic signature mimics the edges of the Nain craton in Labrador, the Rae craton in the Canadian Arctic, and the southwestern Slave, Rae and Hearne cratons in western Canada.

Superior Craton: In the Superior craton, the world's largest contiguous region of Archean crust, the highest velocities occur in the northeastern part of the craton (Fig. 1). They correspond to the geographic position of the Mesoarchean Hudson Bay Terrane which hosts

rocks as old as 4.3 Ga (O'Neil et al., 2008; Boily et al., 2009). The seismic velocity perturbation attains a maximum median value of 7.8 percent above PREM between 115 and 130 km depth (Fig. 2A). The mantle beneath the southern Archean Superior craton is characterized by a slower and shallower velocity domain compared to its northern counterpart (Fig. 1). Tomographic profiles indicate a maximum median value of 4.9 percent above PREM at 105 km compared to 7.6 percent for the northern mantle at the same depth (Fig. 2A, 2B). The boundary between the relative high and low-velocity anomalies corresponds to the major crustal boundary between the Mesoarchean Hudson Bay and the North Caribou Terranes to the north with the Neoproterozoic greenstone belt assemblage (2.7 Ga) to the south (Fig. 1).

Hearne and Rae Cratons: The mantle keel beneath the Rae and Hearne Archean cratons (Fig. 1) corresponds with Mesoarchean basement windows on the surface (MacLachlan et al., 2005) or Paleo-Mesoarchean crustal components in Paleoproterozoic granite suites (van Breemen et al., 2005). The similarity and the continuity of the seismic signature across these two juxtaposed Archean cratons suggest that they share similar Archean mantle, which has been proposed based on trace elements and the ϵ_{Nd} data by Cousens et al. (2001). The S-wave velocity profile underneath this region indicates a colder and/or more depleted mantle than the northern Quebec Superior Province with a maximum median value of 8.3 percent above PREM at depths between 125 and 145 km (Fig. 2C).

Slave Craton: The Slave craton (Fig. 1) hosts world class diamond deposits, leading Canada's third-in-the-world production in terms of diamond value (Kjarsgaard, 2007). The seismic velocity perturbation under this craton is less than the average value observed beneath the adjacent Hearne and Rae Archean cratons with a maximum median value of 7.3 percent above PREM at 135 km compared to 8.3 percent at a similar depth (Fig. 2C, 2D). The highest

velocities do not occur beneath the oldest crust (3.96 - 2.85 Ga) of the Central Slave Superterrane (Helmstaedt, 2009) but under the assemblage of younger rocks (2.72 - 2.55 Ga) of the eastern domain (Kusky, 1989; Bleeker et al., 1999). The velocity perturbations increase progressively with depth and towards the east to connect with the high velocity zone observed beneath the Hearne and Rae cratons (Fig.1).

Wyoming Craton: The Wyoming craton (Fig. 1) hosts rocks of 3.8 to 2.6 Ga (Frost and Frost, 1993). The Archean crust is interpreted to continue under the Phanerozoic sedimentary basins to the northeast (Haussel et al., 1999). The craton was strongly affected by a regional metamorphic event related to the Trans-Hudson Orogen, a remnant of a continental-scale collision belt that juxtaposed a number of Archean cratons during the Paleoproterozoic development of Laurentia (Hoffman, 1989). The lower crust is underplated by a Proterozoic crust and lacks its Archean lithospheric roots (van der Lee and Nolet, 1997; Gorman et al., 2002). This is reflected in the velocity profile as an S-shaped curve as well as a wide range of values and a reduced maximum velocity anomaly of 2.2 percent above PREM at 120 km depth (Fig. 2E).

Seismic Signatures Beneath Under Covered Archean Crust

High velocity perturbations comparable to those observed beneath exposed Archean cratons are also found between or adjacent to them, under younger belts, sedimentary basins, or platforms (Fig. 1). Between the Superior craton and the southern portion of the Hearne craton, the fast seismic anomalies correspond on the surface with the exotic Sask craton (Fig. 1; Collerson et al., 1989; Ansdell et al., 1995). Most of this craton is exposed as windows and includes rocks as old as 3.10 Ga that were affected by magmatism, metamorphism and

deformation during the Trans-Hudson Orogen (Bickford et al., 2005). Seismic and magnetotelluric studies indicate that the Sask craton occupies the majority of the lower crust and extends at least 200 km toward the northeast under the Trans-Hudson Orogen (Corrigan et al., 2005; Garcia and Jones, 2005). The mantle beneath this exotic craton is interpreted to have been detached and replaced by both the Superior and the Hearne mantle lithosphere during final collision of the orogen (Németh et al., 2005). We believe that this interpretation can be extrapolated further to the east and may explain why the widespread arc-related magmatic event in the Trans-Hudson Orogen (Meyer et al., 1992) has no imprint in the upper mantle (Fig. 1).

Alberta: Typical subcratonic fast velocity keels also occur apparently off-craton under sedimentary basins in southwestern (Alberta) and northwestern Canada (Fig. 1). An isolated high-velocity anomaly beneath the Phanerozoic Western Canada Sedimentary Basin in Alberta is herein outlined for the first time. The high-velocity zone is centered underneath the Proterozoic (2.0 - 2.3 Ga) Buffalo Head Terrane (Ross et al., 1991; Carlson et al., 1999a; Ross and Eaton, 2002). It is bounded to the east and south by Rae and Hearne Archean crust, respectively. The center of the keel has the strongest velocity signature of the North American upper mantle with maximum velocity perturbations between 9.5 and 10.1 percent above PREM at depths between 120 and 150 km (Fig. 2F). However, the velocities towards the base of the model show slower mantle values (median of -0.6% at 250 km) compared to the other cratonic roots (Fig. 2). Sm-Nd isotopic data and zircon inheritance, as well as crustal seismic profiles, indicate that the Buffalo Head Terrane was built on an Archean micro-continental edifice (Ross and Eaton, 2002).

Northwest Territories: From the Slave craton to the Alaska border, a continuum in the high velocity perturbations is observed over much of the central Northwest Territories and under the Western Canada Sedimentary Basin (Fig. 1). The average seismic velocity under this area is 6.9 percent above PREM between 100 and 150 km, which is similar to the average beneath the Slave craton (Fig. 2). However, the fastest velocities (maximum median value of 7.1%) are shallower (120 km) compared to the Slave craton (maximum median value of 7.3% at 135 km). The crust overlying the anomaly is regarded as the rocks involved in, or older than the Paleoproterozoic Wopmay orogen, a belt that developed between 2.1 and 1.8 Ga on the western margin of the Archean Slave craton and over an Archean basement (Ross and Eaton, 2002). At the western edge of this high velocity zone, Archean ages have been found in intrusive rocks of the Yukon, suggesting a contamination by crust with an older Archean depleted mantle (Thorkelson et al., 2001). The Cordilleran Tectonic Front closely follows the southern edge of this fast seismic anomaly as well as the Alberta high velocity zone (Fig. 1). We interpret these two seismic anomalies as an Archean mantle rigid-plate buttress that explains the present-day trace of the Cordilleran Tectonic Front and the thin-skinned and thrust-fold tectonics east of it (Cook et al., 2004).

Hudson Bay: In the southern part of Hudson Bay, a strong seismic anomaly occurs under the Paleozoic Hudson Bay and James Bay Lowlands, a platform sequence consisting of flat-lying sedimentary rocks unconformably overlying the Superior craton (Fig. 1; Norris, 1986). The anomaly represents the second-highest velocity perturbation of the tomographic model after Alberta (9.5% above PREM at a depth of 135 km). It corresponds on the surface to the location of the Cape Henrietta Maria Arch structure, which separates the erosional remnants of two adjacent cratonic sedimentary basins (Norris, 1986; Card et al., 1999).

Canadian Arctic: In the southern Canadian Arctic (above latitude 65°N), much of the Archean-Lower Proterozoic metamorphic-plutonic basement is covered by the Cambrian to Devonian Arctic Interior Platform (Fig. 1; Trettin, 1991). The tectonic assemblage in this area is viewed as a set of small Archean cratons welded together in a series of Early Proterozoic orogenies (Hoffman, 1989). In the east, Mesoarchean rocks outcrop on the central portion of Baffin Island and Melville Peninsula where Nd model ages reach 3.7 Ga (Jackson and Berman, 2000). Elsewhere, the Precambrian rocks are exposed as salients and outliers and yield ages from 2.48 to 1.71 Ga with Nd model ages between 3.0 and 2.2 Ga (Kjarsgaard, 1996; Jackson and Berman, 2000). The basement was affected by episodic pulses of thermal uplift (including the thermal plume event responsible for the Mackenzie dyke swarm at 1.2 Ga), rifting between the Late Proterozoic and the Late Devonian, and later by the Innuitian Orogen during Late Silurian to Early Carboniferous (Okulitch et al., 1991; Irvine et al., 2003). Velocities beneath re-worked Archean crust in the Arctic indicate lower-magnitude velocity perturbations (maximum median value of 5.7 % above PREM at 95 km depth) compared to other cratons in Canada (Fig. 2).

In summary, the upper mantle beneath and between exposed Archean cratons is in most places fairly homogeneous and laterally coherent in terms of its high-velocity structures. Such a seismic signature is also found beneath Alberta and the Northwest Territories, west of the Slave craton, over dominantly unexposed Archean-contaminated Proterozoic crust. The lowest-magnitude velocity perturbations (4 to 5 % above PREM) beneath Archean crust are observed at the margin of the North American shield where cratons are not bounded by other cratons.

Architecture of the Archean Mantle

Sections across the tomographic block model show that the mantle beneath Archean cratons is linked by high S-wave velocity structures laterally and vertically, down to 170-200 km on average (Godey et al., 2004). The vertical correspondence between high-velocity perturbations and almost all exposed or subsurface Archean crust, as shown by the above evidence, suggests that the subcratonic mantle in Canada is contiguous in term of velocity structure. To define the volumetric expression of the seismic Archean-only mantle signature, the average S-wave perturbations between depths of 75 and 200 km have been calculated underneath all exposed Archean cratons (Table 1). This range of depth has been chosen because we exclude in the calculation the possible rheological effect of the crust (above 70 km) and the asthenosphere (below 200 km). The result indicates average velocity perturbations varying between 5.7 and 7.0 percent for cratons in Canada (Table 1). The Wyoming craton is distinct with a mean velocity perturbation of 1.7 percent. We use the average velocity perturbations beneath all exposed cratons, except Wyoming, as the lower limit to define the average Archean-only mantle seismic signature (6% in Table 1). The volumetric expression of the 6 percent high-velocity perturbation shell (hereafter “6 percent shell”) is shown in Figure 3. This envelope is believed to represent the highly depleted subcontinental lithospheric mantle beneath Archean cratons of North America.

The 3D solid-body image of the inferred Archean mantle shows that the lithospheric roots beneath cratons are singled out at about 200 km depth (Fig. 3). Archean mantle appears mainly in Canada from Alberta to Québec as a 598 Mkm³ block spanning 3,000 km east-west and 2,300 km north-south. The deepest keels are observed under the Hearne craton and in the

northeastern and northwestern Superior Province, with a maximum depth of 240 and 225 km respectively.

3D Kimberlite Fields Dataset

We have compiled information on 987 kimberlites and 118 lamproites across Canada and the U.S. from literature, government databases, and company reports in order to compare the spatial relationship between kimberlite fields and the tomographic model (Fig. 3; Faure 2010). Kimberlites and lamproites have been distinguished as diamondiferous or non-diamondiferous. Where the information is available, we distinguish between micro-diamonds (<0.85mm in diameter) and macro-diamonds (>0.85mm). The diamond content is unknown for 180 kimberlites. Our estimation is that 57 percent of the kimberlites (567) contain diamonds, whereas only 7 percent of lamproites host diamonds. Of the total amount of kimberlites, 491 kimberlites are located in exposed Archean rocks, of which 267 contain diamonds, 101 are non-diamondiferous, and 123 are classed in the unknown category. Only 3 kimberlites are located in Mesoarchean rocks (Nain craton). From the 496 kimberlites that are hosted in rocks younger than Archean, 300 are diamondiferous, 139 are non-diamondiferous, and 57 are unknown.

Third Dimension of Kimberlite Fields

The formation of lithospheric diamonds (99 percent of all macrodiamonds worldwide) is the result of a reaction with oxidized asthenosphere-derived, silica-bearing, methane-rich fluids and/or low volume, highly volatile, small-degree partial melts that penetrated upward episodically through the base of the subcontinental lithosphere, likely along heterogeneously distributed structural conduits (Malkovets et al. 2007; Stachel and Harris, 2008). Lithospheric diamonds span in age (3.50 to 0.99 Ga) from the Archean to just prior to pipe emplacement,

with the majority having had a long mantle residence history (Gurney et al. 2010). Kimberlite magmas are the mixing products between an asthenospheric melt and the subcontinental lithospheric mantle (Choukroun et al. 2005). Grégoire et al. (2006) proposed that, before reaching the surface and tapping diamonds during the ascent of dykes through the overlying rock via zones of weakness, kimberlitic magmas concentrate and stagnate in low-density fluids, or carbon- and water-rich melt pockets of tens of kilometers in diameter (at a similar scale to the dimension of the kimberlite clusters) just below the Lithosphere-Asthenosphere Boundary (LAB). The presence or the absence of diamonds in kimberlites depends on whether or not the ascending dykes have sampled the primary heterogeneous distribution of diamonds preserved within the mantle domain of diamond stability.

Suites of mantle-derived xenoliths and xenocrysts in mantle-derived intrusions are used to estimate the LAB depth, and indirectly the depth of the magmatic source beneath kimberlite fields at the time of their formation. Major- and trace-element analyses and textures of key mantle minerals (Cr-pyrope garnets, chromites, and olivine) and coexisting xenoliths compared to depth of origin (derived from geothermobarometric analyses) permit the reconstruction of the vertical stratigraphy of the mantle in terms of depletion, metasomatism, deformation and thermal state (O'Reilly et al., 2001; O'Reilly and Griffin, 2006). Archean xenolith suites show low Cr, Ca/Al and Fe/Al values, a high Mg# of olivine (92 to 94), and strongly subcalcic garnets (CaO <4%) depleted in Y, Ga, Zr, Ti, and HREE, consistent with a high (around 30 to 40%) basaltic melt extraction (Gurney, 1984; Boyd, 1989; Griffin et al., 2003). At the base of the depleted Archean lithosphere, the LAB has a pronounced melt-related metasomatic signature defined by: 1) an inflected geotherm; 2) a characteristic Zr, Ti, Y, and Ga (\pm Fe) enrichment in garnets; 3) a high Sr and LREE content in clinopyroxene; 4) an asthenospheric

value of ~ 90 for the Mg# of olivine; and 5) commonly by sheared peridotite xenoliths (Kennedy et al., 2002; Griffin et al., 2004; O'Reilly and Griffin, 2010). When the LAB in the mantle stratigraphy cannot be properly defined on a chemical basis, the deepest xenoliths in geotherm diagrams provide the minimum thickness of the mantle lithosphere.

We have compiled the estimated LAB depth beneath 45 North American kimberlites, lamproites, and volcanic rocks from a number of published xenolith studies (See Table 2 and references cited and Fig. 3 for their location). The petrologic LAB depth shows a good consistency across the cratonic domains with a mean depth of 176 ± 21 km and a maximum depth of 225 km beneath the Snap Lake kimberlite dyke at Lac de Gras (Table 2). The average depth beneath Proterozoic domains in the central and southern U.S. is 155 ± 25 km (Fig. 3).

Distribution of Kimberlite Source Regions Relative to the seismic Archean Mantle

In this section, the 3D spatial relationship of the inferred kimberlite magma source regions at depth is investigated relative to the seismic Archean mantle signature (Fig. 3). Specifically, we would like to highlight regions of correspondence between the 6 percent envelope and the LAB location compiled from xenolith studies (Figs. 3, 4; Table 2). The results show relatively small differences between these two sets of data, well below the range of the resolution of our tomographic model and within the error range for xenolith estimates (Griffin et al., 2004).

In Canada, all kimberlite fields occur within 400 km (inside or outside) of the 6 percent shell (Fig. 3). We estimate that 65 percent of North American kimberlites (640) are located above the seismic Archean mantle envelope, from which 81 percent (419) are diamondiferous (86 kimberlites host macro-diamonds) if we exclude the 121 kimberlites classified in the

unknown category for their diamond content. The proportion of diamondiferous kimberlites outside the 6 percent shell falls to 51 percent (11 kimberlites host macro-diamonds) if the unknown category is excluded. No lamproites are found over the Archean seismic mantle. These latter mantle intrusions closely follow the trend of the western edge of the Alberta keel and the Cordilleran Tectonic Front from the northwestern U.S. to southwestern Canada (Fig. 3).

When comparing the seismic Archean mantle with xenolith studies, we find that among the 45 petrologic LAB control points over the U.S. and Canada, 29 fall above the 6 percent shell and these are only observed in Canada. Overall, the minimum difference in depth between the seismic Archean shell and the petrologic LAB estimated from these 29 control points is less than ± 12 km in average, if we do not take into account the kimberlites of the southwest Slave craton and the 94 to 101 Ma Fort à la Corne area kimberlites, which show a maximum difference of 82 km and 58 km respectively (Fig. 3; Table 2). The difference in depth is 5 km for the Buffalo Hills kimberlite cluster and less than ± 9 km in average for Late Cretaceous-Early Permian Slave kimberlites (Table 2). The inferred magma source for the Attawapiskat kimberlite field lies at less than 12 km above the 6 percent shell, and at less than 19 km below the shell for the Otish kimberlites cluster (Beaver Lake and Portage; Fig. 3; Table 2).

The spatial correspondence or mismatch between the seismic Archean mantle envelope and the kimberlitic magma sources at depth is more evident when the entire kimberlite population is projected on a LAB surface generated by the interpolation of the 45 LAB control points. In the northern and central Slave craton for example, the string of magma pockets defined by the Tertiary-Cretaceous kimberlites (Lockhart et al., 2004) closely follows the shape of the 6 percent shell between depths of 140 and 205 km (Fig. 4). The exception is the Siluro-Ordovician (435 and 459 Ma; Heaman et al., 2003) southwest kimberlite clusters (Drybones

and Cross Lake kimberlites) that lie at the edge of an inverted cone of slower velocities. In Alberta, inferred kimberlite magma source estimates beneath the Buffalo Head and Birch Hills fields also fit very well with the morphology of the Archean mantle, where each field lies on the west and east sides of the keel respectively (Fig. 4). The Attawapiskat, Wemindji, and Otish inferred magma source regions fall in the steep slope along the southern edge of the Archean mantle envelope following the 160 to 175 km depth interval (Fig. 3). A good correlation is also observed between the 6 percent shell and the inferred kimberlite magma pockets of the Western Churchill province (West side of Hudson Bay), where a difference in depth of less than 7 km is calculated (Fig. 3; Table 2).

Discussion

The architecture of the Archean cratonic keels constructed with our tomographic model compares well with the average estimates from local and higher resolution tomographic models in Canada, and with other deep geophysical investigation techniques or geologic interpretations. However, we cannot explain all of the relationships between the geological features observed on the surface and the mantle seismic signatures, probably because the resolution of our model is not fine enough and/or the velocity contrast of some mantle domains is too low to detect some geological features such as fault zones or thin crustal boundaries. An additional complication is produced by poor knowledge about crust-mantle coupling relationships in many parts of the Precambrian core of North America.

Comparison with Local Tomographic Models, Deep Geophysical Results, and Geology

Slave: Beneath the Slave craton, the tomographic model indicates that the 6 percent shell deepens from north to south and from west to east where the root reaches a maximum of 205 km depth in the eastern part of Lac de Gras (Fig. 4). This root morphology is in agreement with magnetotelluric studies, broadband teleseismic data and geological models that indicate a thickening of the lithosphere toward the centre and southeast of the Slave craton, with a maximum LAB depth estimate of ~190-210 km (Bostock, 1997; Jones et al., 2003; Snyder and Bruneton, 2007; Snyder and Grütter, 2010). Moreover, our model shows that the keel of the Slave continues to deepen towards the southeast where it connects with the Rae craton root at an ultimate depth of 240 km. The 3D morphology of the 6 percent shell beneath the Slave craton is likely caused by eastward-directed subduction during the late Archean (Helmstaedt, 2009), or during the Paleoproterozoic Wopmay Orogen (Snyder and Grütter, 2010). The sharp ultra-depleted harzburgite conductive layer observed between 80 and 145 km by Griffin et al. (1999) and Jones et al. (2003) and the multiple underthrust layers constituting the bottom of the Slave lithospheric mantle (Snyder and Grütter, 2010) are not recognized in the tomographic model (Fig. 2D), probably because the velocity contrast of these layers is too low to be perceptible.

The 6 percent shell also clearly shows a rapid thinning of the cratonic mantle lithosphere from the central Slave toward the southwest (Figs. 3, 4). The Ordovician (435-459 Ma) southwest Slave kimberlites (Heaman et al., 2003) occur in this area of slower velocity perturbations (Fig. 4). The mismatch between the 6 percent shell and the inferred magma pockets at depth indicates that diamondiferous kimberlites were emplaced prior to the modification of the cratonic keel.

Alberta: The entire keel morphology beneath Alberta is imaged for the first time as an ovoid body measuring 1,500 km in length, 800 km in width and 185 km in depth, with the long axis trending NW-SE, parallel to and bounded on the west by the Cordilleran Tectonic Front (Figs. 3, 4). Shragge et al. (2002) recognize high velocities beneath much of the southern Hearne Province to a depth of 200 km and suggested that the Hearne lithosphere represents an ancient and rigid lithosphere. The depth of the keel in our model (185 km) is almost equal to xenolith barometric estimates (Table 2; Aulbach et al., 2004) and correlates well with the 200 km depth estimates from a long period magnetotelluric study (Türkoğlu et al., 2009). The garnet geochemistry of mantle xenoliths from the Buffalo Hills kimberlites (88-86 Ma) suggests that the mantle is Archean with a cold conductive paleogeotherm (38-39 mW/m²) but was metasomatized during Paleoproterozoic rifting of the Buffalo Head Terrane from the neighboring Rae Province to the east (Aulbach et al., 2004). This may explain why the Alberta keel is shallower compared to the Slave or Superior seismic signatures and why it is almost isolated from the Hearne and Rae cratons to the east (Figs. 3, 4). The parallelism between the Cordilleran Tectonic Front and the western edge of the keel as well as its northeast dip suggest that a significant thermal and/or mechanical interaction on the west side occurred, most likely during the Laramide orogeny (~75-45 Ma). Geochemical studies of xenoliths from the Cross kimberlite, which is located 150 km SW of the Alberta keel, confirm that the kimberlite sampled little if any Archean lithosphere (Figs. 1, 4; Canil et al., 2003).

Fort à La Corne: The 103-95 Ma Fort à la Corne kimberlite field (Heaman et al., 2003) lies over a shallow (115 km depth) seismic Archean mantle (Figs. 3, 4). Xenolith studies indicate that the kimberlite magmas were generated at about 180 km depth (Griffin et al., 2004). The inferred locus of magma generation at depth lies centered on an inverted conical

low-velocity anomaly (Fig. 3). The low-velocity seismic zone beneath this area is in agreement with the local seismic tomography of Bank et al. (1998) who interpreted this signature as the footprint of a plume event that affected the area of Fort à la Corne in the Cretaceous.

Northwest Territories: The high-velocity anomaly under the Northwest Territories (Fig. 1) has previously been recognized with a lower resolution by Frederiksen et al. (2001) who reported its prolongation further to the west beneath central Alaska and below 150 km depth. The existence of an Archean mantle signature west of the Slave craton and below ancestral North America is debatable. The seismic response of the upper mantle between 100 and 150 km in this region is fairly similar to the mantle signature beneath the Slave craton (Fig. 2). However, the absence of a deep and refractory keel like other cratonic cores in Canada and the flat layered bottom of the 6 percent shell under the Northwest Territories (Fig. 3) suggest the presence of a warmer and/or less depleted or more melt-metasomatized Proterozoic mantle comparable to the Alberta keel (Fig. 2).

Arctic: In the Canadian Arctic, our model agrees with previous observations of Frederiksen et al. (2001) who show a mixed zone of contrasting seismic signatures at 100 and 150 km depth between parallels 65°N and 70°N. In the central and eastern part of this zone, the 6 percent dVs envelope images a remnant 240 km depth V-shaped keel (Fig. 4). North of this remnant keel, xenoliths from the 94-103 Ma old Somerset Island kimberlites indicate that the mantle is much less depleted than typical Archean mantle (Heaman et al., 2003; Irvine et al., 2003). Trace-element isotopic data and Re depletion model ages (TRD) indicate that the lithosphere beneath Somerset Island was stabilized at 2.8 Ga and is stratified, with a lower layer metasomatized during Proterozoic tectonothermal events related to the Taltson-Thelon orogen (Fig. 1; Schmidberger and Francis, 2001; Schmidberger et al., 2001; Irvine et al., 2003).

In northwest Hudson Bay and beneath the Rae craton (Fig. 1), the low-velocity anomaly corresponds to a large negative free air gravity anomaly caused by the influence of large scale convective downwelling within the mantle (Peltier et al., 1992; Hanne et al., 2004). The footprint of this mantle convection is visible on Figures 3 and 4.

Central U.S.: In the mid-continental region of the central U.S., a series of interconnected shallow limbs of high velocity structures is depicted in 3D by the 6 percent shell (Fig. 3). The high velocity signature is comparable to the cratonic lithospheric structure in Canada and suggests the presence of an Archean mantle beneath the thick Mesozoic and Cenozoic marine and stream deposits of the Central Plains (Fig. 1). However, the complexity of the seismic response indicates that the region was affected by tectonothermal events during and after the Proterozoic (van Schmus et al., 1996). For example, the surface expression of the Mid-Continental Rift System (van Schmus and Hinze, 1985) for the most part mimics the morphology of the 6 percent shell (Figs. 1, 3).

Superior: The Superior craton clearly shows two distinct seismic domains separated by a sharp vertical E-W oriented discontinuity in the velocities (Figs. 1, 5). The northern domain is characterized by high velocity perturbations and a 225 km depth keel centered beneath the Mesoarchean Hudson Bay Terrane (Boily et al., 2009). It is noteworthy that the smallest greenstone belts of the craton fit the morphology of this stiff velocity root (Faure et al., 2008). The southern domain corresponds to a low E-W trending velocity channel that is seismically 30 percent slower compared to the northern domain (Fig. 2). Previous regional and local tomographic models have recognized this anomalous zone (van der Lee and Nolet, 1997; Rondenay et al., 2000; van der Lee, 2002). Xenolith studies indicate that the mantle underlying the southern Superior craton is anisotropic and layered compared to the northern part (Griffin et

al., 2004; Scully et al., 2004). The mantle has a more fertile lherzolite component to a depth of 120-140 km compared to the typical Archean mantle. Lower down, the mantle has an abundance of depleted lherzolites and a strong signature of melt-related metasomatism typical of a Proterozoic mantle.

Many authors have interpreted the low-velocity anomaly in the southern Superior craton as a chemical heterogeneity related to the passage of the Cretaceous Great Meteor Hotspot, the last thermal event which affected the upper mantle beneath the southern Superior craton (van der Lee and Nolet, 1997; Rondenay et al., 2000; Frederiksen et al., 2001; Eaton and Frederiksen, 2007). However in our model, the low-velocity zone is more spatially correlated to Neoproterozoic greenstone belts and specific tectonic events of the southern Superior (Fig. 5). The lowest velocities in this part of the craton are centered beneath the Archean Wabigoon and Abitibi Sub-Provinces, the latter representing the largest greenstone belt in the world and the youngest greenstone belt of the Superior craton. We believe that the cause of the seismic signature in the southern Superior craton is not attributed to a unique factor but to a succession of tectonothermal events spanning from the Archean to the Cretaceous. The early modification of the mantle by the formation of greenstone belts in the Neoproterozoic produced a permanent scar that was subsequently reused during younger tectonothermal events to produce the current seismic response. The originally diamondiferous mantle of the Wabigoon and Abitibi Sub-Provinces (Stachel et al. 2006) is thought to have been modified first in Late Archean by subduction-dominated processes even though mantle plumes constantly affected the Abitibi evolution (Daigneault et al., 2004). The traces of at least two Archean north-dipping subduction zones are clearly visible in the tomographic model at 100 km depth, outlining the lowest velocity zone of the Superior Province (Fig. 5; Ludden and Hynes, 2000; Sol et al., 2002;

White et al., 2003). The 1.9 Ga transcrustal Kapuskasing Structural Zone (Percival and West, 1994) crosscuts and disturbs the center of this low velocity zone implying that the mantle was already modified by that time (Fig. 5).

Based on the major and trace element chemistry of garnets from kimberlites and alkaline intrusions, Scully et al. (2004) proposed that the mantle metasomatism in the southern Superior Province is contemporaneous to the 1.1 Ga Mid-continental Rift system (Figs. 3, 5). This major continental rift certainly had a role in the modification of the mantle lithosphere. However, we think that the intrusions belonging to the widespread carbonatite province in Ontario and southern Québec (Sage, 1991; Woolley and Kjarsgaard, 2008) also had an influence in the thermal/compositional modification of the mantle since the Late Archean (Fig. 5). The carbonatite magmatism is a product of metasomatized mantle generated at a depth of ~100 km (Wallace and Green, 1988; Harmer et al., 1998). It was active in this area during five major periods: 2,690-2,480 Ma, 1,890-1,635 Ma, 1,270-880 Ma, 640-560 Ma, and 190-120 Ma (Woolley and Kjarsgaard, 2008). The outline of the carbonatite province closely mimics the lowest-velocity fingerprint at 100 km depth and almost all carbonatites occur outside the 6 percent shell (Fig. 5). This strong spatial relationship with seismic signature suggests that this long period of episodic mantle magmatism has permanently changed the composition of the upper mantle as demonstrated by xenocryst mantle stratigraphy (Scully et al., 2004).

Implications for Diamond Exploration

The North American subcontinental lithosphere is considered relatively homogeneous in terms of rock type distribution (Griffin et al., 2004). The domain characterized by velocities equal to or greater than 6 percent above PREM is assumed to be representative of a chemically

highly depleted, peridotitic and cold refractory Archean mantle. Using a joint inversion of seismic velocities and density (gravity) perturbations, Godey et al. (2004) estimate that the North American craton is colder than average and depleted in iron down to a depth of 230 km. The maximum iron depletion and temperature anomaly are located within the Archean cratonic shell and beneath the Superior craton and Hudson Bay at 100 km depth with a difference in temperature of -170°C and a depletion of -4 percent Fe compared to the model average. The 6 percent shell also represents a good estimation of the petrologic LAB topography, at least for depths below 145 km, i.e. the minimum depth from xenolith estimates that lie over or cross-cut the Archean mantle shell (Table 2). The spatial coincidence between kimberlitic magma sources inferred from xenolith datasets and the Archean seismic shell indicates that the mantle has not suffered significant compositional and thermal changes and was not subject to major destructive mantle events since its stabilization in the Archean.

The small contrast in seismic velocities in the upper mantle between individual Archean craton roots (from 50 to 150 km depth approximately), as illustrated by our model as well as by the higher-resolution model of Darbyshire and Eaton (2010) between the Hearne and Superior cratons (Hudson Bay area), suggests that little or no Proterozoic mantle is preserved at the boundaries between amalgamated cratons. It is suggested that, before their amalgamation during the Paleoproterozoic, cratons acquired an iceberg-like morphology during earlier continental breakup (refer to morphology of the Slave mantle in Fig. 4 and the mantle architecture shown in eastern Canada in Fig. 3). The >300 km extension of the African Congo craton mantle root under the Atlantic is a preserved analogue of this shape (Begg et al., 2009). The collision between two cratons with this morphology results in the appearance of isolated cratons on surface, but the margins of Archean roots are joined together at depth. Proterozoic

mantle wedges may be coupled directly beneath the crust of these mobile belts, but we believe that the majority of the Proterozoic subcontinental lithospheric mantle has been recycled during orogenic processes in the asthenosphere due to its higher density and/or because it was flanked by layers external to Archean cratonic core mantle below 150 km depth. Based on a similar approach to our study in Africa, Begg et al. (2009) also proposed that post-Archean mantle rarely survives the collision/accretion process. In contrast, the edges of cratons that are not in close proximity with another Archean craton but rather with Proterozoic or younger belts, preserved the typical and characteristic lower-velocity signatures of continental margins. An implication of this interpretation is that the regions between the adjacent Slave, Hearne and Superior cratons might be considered for diamond potential even though they are separated by overlying Proterozoic crust.

The diamond potential of a region also has to be considered carefully since the timing of kimberlitic intrusions relative to the age of the mantle modifications is in most cases diachronous. We present the Superior craton as a typical example of this challenge because this Archean craton has a surface area more than seven times that of the Slave craton and it hosts nearly 150 kimberlite pipes or dykes concentrated in its central and southern parts (Fig. 5). The emplacement of kimberlites is contemporaneous to the last three periods of carbonatite magmatism: Desmaraisville, Kyle Lake, and Whitefish Lakes kimberlites cluster at ~1100 Ma (Sage, 2000; Kaminsky et al., 2002); the Wemindji and Otish kimberlites cluster at 630 and 550 Ma respectively (Mitchell and Letendre, 2003; Birkett et al., 2004); and the Attawapiskat, Kirkland Lake, Timiskaming and Lake Ellen kimberlites lie between 190 and 125 Ma (Fig. 5; Heaman and Kjarsgaard, 2000). Kimberlites of all ages are found in both the seismically-distinct southern and central Superior craton.

As previously mentioned, the southern part of the Superior craton lies outside the bounds of the 6 percent shell in velocity anomaly, and is interpreted to have been affected periodically by thermomechanical modifications since the Archean. The first modification of a Mesoproterozoic mantle occurred during the Neoproterozoic by the formation of greenstone belts and related mantle plumes and subduction (Daigneault et al., 2004; Wyman and Kerrich, 2009). Later modifications occurred periodically since the Proterozoic with the emplacement of widespread carbonatite and other mantle-derived igneous rocks, which ended in the Cretaceous with the passage of the Great Meteor Hot Spot. The Proterozoic and younger magmatic events signify a progressive thinning of the Archean mantle by the sporadic ascent of the asthenosphere. Consequently, the diamond stability field has been partially or totally destroyed by thermal and/or chemical processes at different times and in various areas of the upper mantle. The global and permanent deterioration of the diamond stability field through time implies that kimberlites that have passed across the mantle during or after an episode of metasomatism have less chance of intercepting preserved pockets of diamonds. This explains why only 23 percent of the 96 kimberlites in the southern Superior are diamondiferous and why the proportion of macro diamonds is very low; only 7 kimberlites contain at least one macro diamond.

In contrast, 78 percent of the 55 kimberlites of the central Superior craton, including the Victor mine at Attawapiskat and the Renard feasibility mine project in the Otish mountains, are located in the typical cold and depleted Archean shell, contain abundant diamonds with a high proportion of macro and gem-quality diamonds and have a strong harzburgitic signature (Grütter et al., 2006).

New Model for Diamondiferous Kimberlites

Kennedy (1964), followed by Clifford (1966) and Janse (1984), showed that kimberlites are confined to older and stable cratons. Schematic models from Mitchell (1991), Haggerty (1994) and Taylor et al. (1994) placed the kimberlite magma generation sites and ascent paths from the upper mantle to the surface in the central cores of cratons and at their margins. Based on the global tomographic model of Grand (1994), Griffin et al. (2004) showed that most diamondiferous kimberlites in North America are located around a broad cratonic core. Begg et al. (2009) and Griffin et al. (2009) also showed that African kimberlites tend to cluster around peripheries of high seismic velocity areas. Our tomographic model further refines these hypotheses. Sections across the tomographic model demonstrate that most kimberlites underlain by Archean mantle are not above the deepest parts of the cratons but rather in areas of abrupt changes and steep slopes around the deepest cratonic keels (180 to 200 km depth) of a few hundred kilometers in diameter (Figs. 3, 6). Compared to the flat topography of the deep cratonic centers or some linked shallower plateaus between keels, slope angles under the peripheral kimberlite fields vary between 4 and 23 degrees (11 degrees on average based on sections of Fig. 6), indicating much steeper slopes in areas of kimberlitic magma departures and ascension. Moreover, all existing diamond mines, future mines, and prefeasibility mine projects (except Fort à la Corne) in Canada are located in regions corresponding to depths between 162 and 198 km (average 187 km) when they are projected vertically down to intercept the 6 percent shell (Figs. 3, 6). This interval of depth in the mantle corresponds to depths required for diamond stability (Kennedy and Kennedy, 1976). Thus, the regions in the mantle where gem-quality diamonds should be stocked and stable since their formation are broadly defined here

for the first time. The projection of these regions to the earth's surface represents regional areas of high prospectivity (Fig. 3).

The distribution of diamondiferous kimberlites relative to the 6 percent shell leads us to propose a new model for diamondiferous kimberlite localization and formation. Based on our tomographic model, none of the deepest keels (>200 km) have been sampled either by known kimberlites (Figs. 3, 6) or by other deep mantle source magmas. Consequently, the age and petrologic nature of the entire upper mantle column forming these deepest keels is not fully constrained. However, all five keels >200 km depth are located beneath exposed pieces of Paleo-Mesoarchean crust (Fig. 1). It is proposed that these higher velocity zones represent Paleo-Mesoarchean highly depleted dunite/harzburgitic nuclei, the “pristine Archean mantle” of Griffin et al. (2009), as proposed for the early South African mantle (Shirey et al., 2004). The 6 percent shell also reveals that most keels are flat-bottomed, as imaged beneath Lac de Gras (800 x 500 km²), Alberta (600 x 250 km²), and the Superior craton (400 x 300 km²) in central Québec (Figs. 4, 6). We interpret the flat topography as the result of erosion and dragging at the base of the keels. The relative plate motion between lithospheric and asthenospheric mantles may cause a concentration of simple shear at the base to lead to a lattice-preferred orientation of minerals (mostly porphyroclastic olivine), which rotates toward the horizontal flow plane with increasing strain (Bokermann and Silver, 2002; Kennedy et al., 2002).

We propose in a schematic model that protokimberlite magmas are stable and stagnate at >200 km depth in areas of flat basal mantle topography beneath the deepest cratonic keels (Fig. 7). The high degree of rigidity, the anhydrous composition, and the horizontal fabric that characterizes the bottom of the keels act as a rheological cap for kimberlitic magma ascension.

The vapor, carbonic liquid, and magmas generated by a heating event (e.g. plume or ascent of a hotter current of mantle asthenosphere) that accumulate and stagnate beneath the flat base of the keels, at the LAB interface, form unstable pockets that migrate by excess of pressure laterally and upward along zones of steeper slopes. The slow migration of magma pockets towards shallower levels along the LAB initiates depressurization. This mechanism is the starting point for a rapid ascension of magma through the mantle. The boundary between older, harzburgitic, and rheologically-stiffer deep mantle keels and surrounding Neoproterozoic subducted-accreted eclogitic mantle may be a preferential lithospheric channel for ascending magmas via sub-vertical zones of weakness.

Conclusion

The architecture of North American cratonic roots has been defined for the first time in 3D using a high-resolution tomographic model. The correspondence between large scale geological, geophysical and petrological data on the surface and at depth permits imaging **of* the geometry of inferred cold and depleted Archean mantle. In particular, there is an encouraging agreement between xenolith data and the base of the Archean seismological lithosphere which also corresponds to the petrologic definition of the LAB topography. Each of the five principal North American cratons has its own seismic response corresponding to its tectonothermal evolution, and small contrasts in the seismic signature are observed, except for the Wyoming craton. Relatively cold and depleted mantle is not necessarily observed beneath all exposed Archean rocks, and not all parts of exposed cratons have a typical Archean seismic signature at depth. Our model constrains the dimensions of the mantle metasomatism in the southern Superior craton and highlights the higher diamond potential of the central part of the world's largest craton. The new geological interpretation of the southern Superior craton

lithosphere suggests that diamond potential diminishes with rejuvenation of mantle-derived magmatism from the Late Archean to the Cretaceous.

An important conclusion of this study is that diamondiferous kimberlites are not located over the deepest part of the cratonic roots, but around sub-spherical, steep, and deep (>200 km) cratonic keels of a few hundred kilometers in diameter. The starting point for kimberlite magma ascension to the surface originates from these areas, at depths between 160 and 200 km. This interval of depth delineates the regions of the upper mantle where diamonds should have been stable since the Archean, and over which all existing diamond-producing mines and future mines in Canada are located, allowing constraints for new exploration areas. Deep keels (>200 km) may represent the core of Paleo-Mesoarchean rheologically-stiffer nuclei against which Neoproterozoic juvenile terranes have been accreted. Dragging at their bases has produced a rheological boundary that may explain why there are no kimberlites over these cratonic cores.

Acknowledgments

We are grateful to Fiona Darbyshire and Heather Short for their thoughtful reviews that helped to improve the manuscript. The reviewers William L. Griffin and Wouter Bleeker are thanked for their constructive comments and suggestions that improved the final version of the paper. This research was funded by the Economic Development Agency of Canada for the Regions of Québec (DEC-CED Canada), the Ministère des Ressources Naturelles et Faune (MRNF) and Développement Économique, Innovation et Exportation (MDEIE) of Québec, and private exploration companies. We also thank I. Lapointe for editing the earlier version of the manuscript and C. Dallaire for help with figures.

References

Afonso, J.C., and Ranalli, G., 2004, Crustal and mantle strengths in continental lithosphere: is the jelly sandwich model obsolete?: *Tectonophysics*, v. 394, p. 221-232.

Alsina, D., Woodward, R.L., and Snieder, R., 1996, Shear wave velocity structure in North America from large-scale waveform inversions of surface waves: *Journal of Geophysical Research*, v. 101, p. 15969-15986.

Anderson, D.L., Tanimoto, T., and Zhang, Y.S., 1992, Plate tectonics and hotspots: The third dimension: *Science* v. 256, p. 1645-1650.

Ansdell, K.M., Lucas, S.B., Connors, K.A., and Stern, R.A., 1995, Kiseeynew meta-sedimentary gneiss belt, Trans-Hudson Orogen (Canada): back-arc origin and collisional inversion: *Geology*, v. 23, p. 1039-1043.

Arndt, N.T., Coltice, N., Helmstaedt, H., and Gregoire M., 2009, Origin of Archean subcontinental lithospheric mantle: some petrological constraints: *Lithos* v. 109, p. 61-71.

Artemieva, I.M., 2009, The continental lithosphere: Reconciling thermal, seismic, and petrologic data: *Lithos*, v. 109, p. 23-46.

Artemieva, I.M., and Mooney, W.D., 2001, Thermal thickness and evolution of Precambrian lithosphere: a global study: *Journal of Geophysical Research*, v. 106, p. 16387- 16416.

Artemieva, I.M., and Mooney, W.D., 2002, On the relations between cratonic lithosphere thickness, plate motions, and basal drag: *Tectonophysics*, v. 358, p. 211-231.

Aulbach, S., Griffin, W.L., O'Reilly, S.Y., and McCandless, T.E., 2004, Genesis and evolution of the lithospheric mantle beneath the Buffalo Head Terrane, Alberta (Canada): *Lithos*, v. 77, p. 413-451.

Bank, C.G., Bostock, M.G., and Ellis, R.M., 1998, Lithospheric mantle structure beneath the Trans-Hudson Orogen and the origin of diamondiferous kimberlites. *Journal of Geophysical Research*, v. 103, p. 10,103-10,114.

Bedle, H., and van der Lee, S., 2009, S velocity variations beneath North America: *Journal of Geophysical Research*, v. 114, B07308, doi:10.1029/2008JB005949.

Begg, G.C., Griffin, W.L., Natapov, L.M., O'Reilly, S.Y., Grand, S.P., O'Neill, C.J., Hronsky, J.M.A., Poudjom Djomani, Y., Swain, C.J., Deen, T., and Bowden, P., 2009, The lithospheric architecture of Africa: Seismic tomography, mantle petrology, and tectonic evolution: *Geosphere*, v. 5, p. 23–50.

Bickford, M.E., Mock, T.D., Steinhart III, W.E., Collerson, K.D., and Lewry, J.F., 2005, Origin of the Archean Sask craton and its extent within the Trans-Hudson orogen: evidence from Pb and Nd isotopic compositions of basement rocks and post-orogenic intrusions. *Canadian Journal of Earth Sciences*, v. 42, p. 659-684.

Birkett, T.C., McCandless, T.E., and Hood, C.T., 2004, Petrology of the Renard igneous bodies: host rocks for diamond in the northern Otish Mountains region, Quebec: *Lithos*, v. 76, p. 475-490.

Bleeker, W., Ketchum, J.W.F., Jackson, V.A., and Villeneuve, M., 1999, The Central Slave Basement Complex. Part I: its structural topology and autochthonous core: *Canadian Journal of Earth Sciences*, v. 36, p. 1083-1109.

Boily, M., Leclair, A.D., Maurice, C., Bédard, J.H., Berclaz, A., and David, J., 2009, Paleo- to Mesoarchean basement recycling and terrane definition in the Northeastern Superior Province, Québec, Canada: *Precambrian Research*, v. 168, p. 23-44.

Bokelmann, G.H.R., and Silver, P.G., 2002, Shear stress at the base of shield lithosphere: *Geophysical Research Letters*, v. 29, 2091.

Bostock, M.G., 1997, Anisotropic upper-mantle stratigraphy and architecture of the Slave craton: *Nature*, v. 390, p. 392-395.

Boyd, F.R., 1989, Compositional distinction between oceanic and cratonic lithosphere: Earth and Planetary Science Letters, v. 96, p. 15-26.

Boyd, F.R., Gurney J.J., and Richardson S.H., 1985, Evidence for a 150-200 km thick Archaean lithosphere from diamond inclusion thermobarometry: Nature, v. 315, p. 387-389.

Canil, D., Schulze, D.J., Hall, D., Hearn, B.C.Jr., and Milliken, S.M., 2003, Lithospheric roots beneath western Laurentia: the geochemical signal in mantle garnets: Canadian Journal of Earth Sciences, v. 40, p. 1027-1051.

Carbno, G.B., and Canil, D., 2002, Mantle structure beneath the SW Slave craton, Canada: constraints from garnet geochemistry in the Drybones Bay kimberlite: Journal of Petrology, v. 43, p. 129-142.

Card, K.D., Sanford, B.V., and Card, G.M., 1999, Controls on the emplacement of kimberlites and alkali rock-carbonatite complexes in the Canadian Shield and surrounding regions: Exploration and Mining Geology, v. 6, p. 285-296.

Carlson, S.M., Hillier, W.D., Hood, C.T., Pryde, R.P., and Skelton, D.N., 1999a, The Buffalo Hills kimberlites: a newly-discovered diamondiferous kimberlite province in north-central Alberta, Canada: International Kimberlite Conference, 7th, South Africa, 11-17 April 1998, Proceedings, p. 109-116.

Carlson, R.W., Irving, A.J., and Hearn, B.C.Jr., 1999b, Chemical and isotopic systematics of peridotite xenoliths from the Williams kimberlite, Montana: Clues to processes of lithosphere formation, modification and destruction: International Kimberlite Conference, 7th, South Africa, 11-17 April 1998, Proceedings, p. 90-98.

Choukroun, M., O'Reilly, S.Y., Griffin, W.L., Pearson, N.J., and Dawson J.B., 2005, Hf isotopes of MARID (mica-amphibole-rutile-ilmenite-diopside) rutile trace metasomatic processes in the lithospheric mantle: *Geology*, v. 33, p.45-48.

Clifford, T.N., 1966, Tectono-metallogenic units and metallogenic provinces of Africa: *Earth and Planetary Science Letters*, v. 1, p. 421-434.

Clowes, R.M., Cook, F.A., Green, A.G., Keen, C.E., Ludden, J.N., Percival, J.A., Quinlan, G.M., and West, G.F., 1992, Lithoprobe: new perspectives on crustal evolution: *Canadian Journal of Earth Sciences* v. 29, p.1813-1864.

Collerson, K.D., van Schmus, R.W., Lewry, J.F., and Bickford, M.E., 1989, Sm-Nd isotopic constraints on the age of the buried basement in central and southern Saskatchewan: implications for diamond exploration: Summary of Investigations 1989, Saskatchewan Geological Survey, Miscellaneous Report 89-4, p. 168-171.

Cook, F.A., Clowes, R.M., Snyder, D.B., van der Velden, A.J., Hall, K.W., Erdmer, P., and Evenchick, C.A., 2004, Precambrian crust beneath the Mesozoic northern Canadian Cordillera discovered by Lithoprobe seismic reflection profiling: *Tectonics*, v. 23, p. TC2010.

Coopersmith, H.G., Mitchell, R.H., and Hausel, W.D., 2003, Kimberlites and lamproites of Colorado and Wyoming, USA: International Kimberlite Conference, 8th, Canada, 16-21 June 2003, Colorado and Wyoming Field Trip Guidebook, 24 p.

Corrigan, D., Hajnal, Z., Németh, B., and Lucas, S.B., 2005, Tectonic framework of a Paleoproterozoic arc-continent to continent-continent collisional zone, Trans-Hudson Orogen, from geological and seismic reflection studies: *Canadian Journal of Earth Sciences*, v. 42, p. 421-434.

Cousens, B.L., Aspler, L.B., Chiarenzelli, J.R., Donaldson, J.A., Sandeman, H., Peterson, T.D., and LeCheminant, A.N., 2001, Enriched Archean lithospheric mantle beneath western Churchill Province tapped during Paleoproterozoic orogenesis: *Geology*, v. 29, p. 827-830.

Daigneault, R., Mueller, W.U., and Chown E.H., 2004, Abitibi greenstone belt plate tectonics: the diachronous history of arc development, accretion and collision, *in* Eriksson, P., Altermann, W., Nelson, D., Mueller, and W., Catuneanu, O., eds., *Tempos of events in Precambrian time*: London, Elsevier, *Developments in Precambrian Geology* 12, p. 88-102.

Darbyshire, F.A., and Eaton, D.W., 2010, The lithospheric root beneath Hudson Bay, Canada from Rayleigh wave dispersion: No clear seismological distinction between Archean and Proterozoic mantle: *Lithos*, doi:10.1016/j.lithos.2010.04.10

Darbyshire, F.A., Eaton, D.W., Frederiksen, A.W., and Ertolahti, L., 2007, New insights into the lithosphere beneath the Superior Province from Rayleigh wave dispersion and receiver function analysis: *Geophysical Journal International*, v. 169, p. 1043-1068.

Doyle, P.M., Gurney, J.J., and le Roex, A., 2003, Xenoliths from the Arnie, Misery and Pigeon kimberlites, Ekati Mine, NWT, Canada: International Kimberlite Conference, 8th, Canada, 22-27 June 2003, Extended Abstracts.

Durrheim, R.J., and Mooney, W.D., 1994, Evolution of the Precambrian Lithosphere: Seismological and geochemical constraints: *Journal of Geophysical Research*, v. 99, p. 15,359-15,374.

Dziewonski, A.M., and Anderson, D.L., 1981, Preliminary reference Earth model: *Physics of the Earth and Planetary Interiors*, v. 25, p. 25,297-25,356.

Eaton, D.W., and Frederiksen, A., 2007, Seismic evidence for convection-driven motion of the North American plate: *Nature*, v. 446, p. 428-431.

Eggler, D.H., Meen, J.K., Welt, F., Dudas, F.O., Furlong, K.P., McCallum, M.E., and Carlson, R.W., 1988, Tectonomagmatism of the Wyoming Province: Colorado School of Mines Quarterly, v. 83, p. 25-40.

Faure, S, 2010, World Kimberlites CONSOREM Database (Version 3): Consortium de Recherche en Exploration Minérale CONSOREM, Université du Québec à Montréal, Numerical Database (<http://www.consorem.ca>).

Faure, S., Daigneault, R., and Godey, S., 2008, Upper mantle architecture of the Archean Superior Province and the implication for the dimension, orientation, metamorphism, and mineralization of the greenstone belts: GAC-MAC Joint Annual Meeting, Program with Abstracts, Québec, p. 55.

Foley, S.F., Buhre, S., and Jacob, D.E., 2003, Evolution of the Archaean crust by delamination and shallow subduction: Nature, v. 421, p. 249-252.

Forte, A.M., and Perry, H.K.C., 2000, Geodynamic evidence for a chemically depleted continental tectosphere: Science, v. 290, p. 1940-1944.

Foster, D.A, Mueller, P.A., Mogk, D.W., Wooden, J.L., and Vogl, J.J., 2006, Proterozoic evolution of the western margin of the Wyoming craton: implications for the tectonic and magmatic evolution of the northern Rocky Mountains. Canadian Journal of Earth Sciences, v. 43, p. 1601-1619.

Frederiksen, A.W., Bostock, M.G., and Cassidy, J.F., 2001, S-wave velocity structure of the Canadian upper mantle: *Physics of the Earth and Planetary Interiors*, v. 124, p. 175-191.

Frederiksen, A.W., Miong, S.-K., Darbyshire, F., Eaton, D., Rondenay, S., and Sol, S., 2007, Variations in Lithospheric Thickness Across the Superior Province, Ontario, Canada: Evidence from Tomography and Shear-Wave Splitting: *Journal of Geophysical Research* v. 112, B07318, p. 1-20.

Frost, C.D., and Frost, B.R., 1993, The Archean history of the Wyoming province, *in* Snoke, S.W., Steidtmann, J.R., and Roberts, S.M., eds., *Geology of Wyoming*, Geological Society of Wyoming, Memoir n. 5, pp. 58-76.

Garcia, X., and Jones, A.G., 2005, Electromagnetic image of the Trans-Hudson orogen - THO94 transect: *Canadian Journal of Earth Sciences*, v. 42, p. 479-493.

Godey, S., 2002, Structure of the uppermost mantle beneath North America: Regional surface wave tomography and thermo-chemical interpretation: Published Ph.D. thesis, Utrecht, Netherland, Utrecht University, 122 p.

Godey, S., Snieder, R., Villasenor, A., and Benz, H.M., 2003, Surface wave tomography of North America and the Caribbean using global and regional broad-band networks: phase

velocity maps and limitations of ray theory: *Geophysical Journal International*, v. 152, p. 620-632.

Godey, S., Deschamps, F., and Tramper, J., 2004, Thermal and compositional anomalies beneath the North American continent: *Journal of Geophysical Research*, v.109, B01308, 13 p.

Gorman, A.R., Clowes, R.M., Ellis, R.M., Henstock, T.J., Spence, G.D., Keller, G.R., Levander, A., Snelson, C.M., Buriannyk, M.J.A., Kanasewich, E.R., Asudeh, I., Hajnal, Z., and Miller, K.C., 2002, Deep Probe: imaging the roots of western North America: *Canadian Journal of Earth Sciences*, v. 39, p. 375-398.

Grand, S.P., 1994, Mantle shear structure beneath the Americas and surrounding oceans: *Journal of Geophysical Research*, v. 99, p. 11,591-11,621.

Grégoire, M., Rabinowicz, M., and Janse, A.J.A., 2006, Mantle mush compaction: a key to understand the mechanisms of concentration of kimberlite melts and initiation of swarms of kimberlite dykes: *Journal of Petrology*, v. 47, p. 631-646.

Griffin, W.L., Doyle, B.J., Ryan, C.G., Pearson, N.J., O'Reilly, S.Y., Davies, R., Kivi, K., van Achterbergh, E., and Natapov, L.M., 1999, Layered mantle lithosphere in the Lac de Gras Area, Slave Craton: Composition, structure and origin: *Journal of Petrology*, v. 40, p. 705-727.

Griffin, W.L., O'Reilly, S.Y., Abe, N., Aulbach, S., Davies, R.M., Pearson, N.J., Doyle, B.J., and Kivi, K., 2003, The origin and evolution of Archean lithospheric mantle: Precambrian Research, v. 127, p. 19-41.

Griffin, W.L., O'Reilly, S.Y., Doyle, B.J., Pearson, N.J., Coopersmith, H., Kivi, K., Malkovets, V., and Pokhilenko, N., 2004, Lithosphere mapping beneath the North American plate: Lithos, v. 77, p. 873-922.

Griffin, E.L., O'Reilly, S.Y., Afonso, J.C., and Begg, G.C., 2009, The Composition and Evolution of Lithospheric Mantle: a Re-evaluation and its Tectonic Implications: Journal of Petrology, v. 50, p. 1185-1204.

Grütter, H., Latti, D., and Menzies, A., 2006, Cr-Saturation arrays in concentrate garnet compositions from Kimberlite and their use in mantle barometry: Journal of Petrology, v. 47, p. 801-820.

Gurney, J.J., 1984, A correlation between garnets and diamonds in kimberlite, *in* Harris, P.G., and Glover, J.E., eds., Kimberlite occurrence and origin: a basis for conceptual models in exploration, Geology Department and University Extensions, University of Western Australia, Publication n. 8, p. 143-146.

Gurney, J.J., Helmstaedt, H.H., le Roex, A.P., Nowicki, T.E., Richardson, S.H., and Westerlund, K.J., 2005, Diamonds: crustal distribution and formation processes in time and

space and an integrated deposit model, *in* Hedenquist, J.W., Thompson, J.F.H., Goldfarb, R.J., and Richards, J.P., eds. ECONOMIC GEOLOGY, 100TH ANNIVERSARY VOLUME, p. 143-178.

Gurney, J.J., Helmstaedt, H.H., Richardson, S.H., and Shirey, S.B., 2010, Diamonds through Time: ECONOMIC GEOLOGY, v. 105, pp. 689- 712.

Haggerty, S.E., 1994, Superkimberlites: a geodynamic diamond window to the Earth's core: Earth and Planetary Science Letters, v. 122, p. 57-69.

Hanne, D., White, N., Butler, A., and Jones, S., 2004, Phanerozoic vertical motions of Hudson Bay: Canadian Journal of Earth Sciences, v. 41, p. 1181-1200.

Harmer, R.E., Lee, C.A., and Eglington, B.M., 1998, A deep mantle source for carbonatite magmatism: evidence from the nephelinites and carbonatites of the Buhera district, SE Zimbabwe: Earth and Planetary Science Letters, v. 158, p. 131-142.

Haussel, W.D., Kucera, R.E., McCandless, T.E., and Gregory, R.W., 1999. Mantle-derived breccias pipes in the southern Green River Basin of Wyoming: International Kimberlite Conference, 7th, South Africa, 11-17 April 1998, Proceedings, p. 348-352.

Heaman L.M., and Kjarsgaard, B.A., 2000, Timing of eastern North American kimberlite magmatism: continental extension of the Great Meteor hotspot track?: *Earth and Planetary Science Letters*, v. 178, p. 253-268.

Heaman, L.M., Kjarsgaard, B.A., and Creaser, R.A., 2003, The timing of kimberlite magmatism in North America: implications for global kimberlite genesis and diamond exploration: *Lithos*, v. 71, p. 153-184.

Helmstaedt, H., 2009, Crust–mantle coupling revisited: The Archean Slave craton, NWT, Canada: *Lithos*, v. 112, p. 1055-1068.

Hoffman, P.F., 1989, Precambrian geology and tectonic history of North America, *in* The geology of North America: an overview, *in* Bally A.W., and Palmer, A.R., Geological Society of America, v. A. p. 447-512.

Humphreys, E.D., and Dueker, K.G., 1994, Western U.S. upper mantle structure: *Journal of Geophysical Research*, v. 99, p. 9615-9634.

Irvine, G.J., Pearson, D.G., Kjarsgaard, B.A., Carlson, R.W., Kopylova, M.G., and Dreibus, G., 2003, A Re-Os isotope and PGE study of kimberlite-derived peridotite xenoliths from Somerset Island and a comparison to the Slave and Kaapvaal cratons: *Lithos*, v. 71, p. 461-488.

Jackson, G.D., and Berman, R.G., 2000, Precambrian metamorphic and tectonic evolution of northern Baffin Island, Nunavut, Canada: *The Canadian Mineralogist*, v. 38, p. 399-421.

Janse A.J.A., 1984, Kimberlites - where and when?, *in* Glover J.E., and Harris, P.G., eds., Kimberlite occurrence and origin: a basis for conceptual models in exploration, Geology Department and University Extension, University of Western Australia, publication n. 8, p. 19-62.

Jones, A.G., Lezaeta, P., Ferguson, I.J., Chave, A.D., Evans, R.L., Garcia, X., and Spratt, J. 2003, The electrical structure of the Slave craton: *Lithos*, v. 71, p. 505-527.

Kaminsky, F.V., Sablukov, S.M., Sablukova, L.I., Shchukin, V.S., and Canil, D., 2002, Kimberlites from the Wawa area, Ontario: *Canadian Journal of Earth Sciences*, v. 39, p. 1819-1838.

Kennedy, W.G., 1964, The structural differentiation of Africa in the Pan-African (+500 m.y.) tectonic episode: Research Institute of African Geology, 8th Annual Report, Leeds University, p. 48-49.

Kennedy, C.S., and Kennedy, G.C., 1976, The equilibrium boundary between graphite and diamond, *Journal of Geophysical Research*, v. 81, p. 2467-2470.

Kennedy, L.A., Russel, J.K., and Kopylova, M.G., 2002, Mantle shear zones revisited: The connection between the cratons and mantle dynamics: *Geology*, v. 30, p. 419-422.

Kjarsgaard, B.A., 1996, Somerset Island kimberlite field, District of Franklin, NWT, *in* LeCheminant, A.N., Richardson, D.G., Dilabio, R.N.W., and Richardson, K.A., eds., *Searching for diamonds in Canada: Geological Survey of Canada, Open File 3228*, p. 61-66.

Kjarsgaard, B.A., 2007, Kimberlite diamond deposits, *in* Goodfellow, W.D., ed., *Mineral deposits of Canada: A synthesis of major deposit types, district metallogeny, the evolution of geological provinces, and exploration methods: Geological Association of Canada, Mineral Deposits Division, Special Publication n. 5*, p. 245-272.

Kolebaba, M., Read, G., Kahlert, B., and Kelsch, D., 2003, Diamondiferous kimberlites on Victoria Island, Canada: a northern extension of the Slave Craton: *International Kimberlite Conference, 8th, Canada, 22-27 June 2003, Extended Abstracts*.

Kopylova, M.G., and Caro, G., 2004, Mantle xenoliths from the southeastern Slave Craton: evidence for chemical zonation in a thick, cold lithosphere: *Journal of Petrology*, v. 45, p. 1045-1067.

Kopylova, M.G., and Russell, J.K., 2000, Chemical stratification of cratonic lithosphere: constraints from the northern Slave craton, Canada: *Earth and Planetary Science Letters*, v. 181, p. 71-87.

Kusky, T.M., 1989, Accretion of the Archean Slave Province: *Geology*, v. 17, p. 63-67.

Levshin, A.L., Ritzwoller, M.H., Barmin, M.P., Villasenor, A., and Padgett, C.A., 2001, New constraints on the Arctic crust and uppermost mantle: surface wave group velocities, Pn and Sn: *Physics of the Earth and Planetary Interiors*, v. 123, p. 185-204.

Lockhart, G., Grutter, H., and Carlson, J., 2004, Temporal, geomagnetic, and related attributes of kimberlite magmatism at Ekati, Northwest Territories, Canada: *Lithos*, v. 77, p. 665-682.

Ludden, J., and Hynes, A., 2000, The Lithoprobe Abitibi-Grenville transect: two billion years of crust formation and recycling in the Precambrian Shield of Canada: *Canadian Journal of Earth Sciences*, v. 37, p. 459-476.

MacKenzie, J.M., and Canil, D., 1999, Composition and thermal evolution of cratonic mantle beneath the central Archean Slave Province, NWT, Canada: *Contributions to Mineralogy and Petrology*, v. 134, p. 313-324.

MacLachlan, K., Davis, W.J., and Relf, C., 2005, U/Pb geochronological constraints on Neoproterozoic tectonism: multiple compressional events in the northwestern Hearne Domain, Western Churchill Province, Canada: *Canadian Journal of Earth Science*, v. 42, p. 85-109.

Malkovets, V.G., Griffin, W.L., O'Reilly, S.Y., and Wood, B.J., 2007, Diamond, subcalcic garnet, and mantle metasomatism: Kimberlite sampling patterns define the link: *Geology*, v. 35, p. 339-342.

Menzies, A., Westerlund, K., Grütter, H., Gurney, J., Carlson, J., Fung, A., and Nowicki, T., 2004, Peridotitic mantle xenoliths from kimberlites on the Ekati Diamond Mine property, NWT, Canada: major element compositions and implications for the lithosphere beneath the central Slave craton: *Lithos*, v. 77, p. 395-412.

Meyer, M.T., Bickford, M.E., and Lewry, J.F., 1992, The Wathaman batholith: An Early Proterozoic continental arc in the Trans-Hudson orogenic belt, Canada: *Geological Society of America Bulletin*, v. 104, p. 1073-1085.

Mitchell, R.H., 1991, Kimberlites and lamproites: primary sources of diamonds: *Geoscience Canada* v. 18, p. 1-16.

Mitchell, R.H., and Letendre, J., 2003, Mineralogy and petrology of the kimberlite from Wemindji, Quebec: International Kimberlite Conference, 8th, Canada, 22-27 June 2003, Extended abstracts.

Mooney, W.D., Laske, G., and Masters, T.G., 1998, Crust 5.1: a global crustal model at 5°×5°: *Journal of Geophysical Research*, v. 103, p. 727-748.

Németh, B., Clowes, R.M., and Hajnal, Z., 2005, Lithospheric structure of the Trans-Hudson Orogen from seismic refraction – wide-angle reflection studies: *Canadian Journal of Earth Sciences*, v. 42, p. 435-456.

Nettles M., and Dziewoński, A.M., 2008, Radially anisotropic shear velocity structure of the upper mantle globally and beneath North America: *Journal of Geophysical Research*, v. 113, B02303, doi:10.1029/2006JB004819.

Norris, A.W., 1986, Review of Hudson Platform Paleozoic stratigraphy and biostratigraphy, *in* Martini, I.P., ed., *Canadian Inland Seas*: New York, Elsevier, p. 494- 503.

Okulitch, A.V., Packard, J.J., and Zolnai, A.I., 1991, Late Silurian-Early Devonian deformation of the Boothia Uplift, *in* Trettin, H.P., ed., *Geology of the Innuitian Orogen and Arctic Platform of Canada and Greenland*: Geological Survey of Canada, *Geology of Canada* no 3, p. 302-307.

O’Neil, J., Carlson, R.W., Francis, D., and Stevenson, R.K., 2008, Neodymium-142 Evidence for Hadean Mafic Crust: *Science*, v. 321, p. 1828-1831.

O’Reilly, S.Y., and Griffin, W.L., 2006, Imaging global chemical and thermal heterogeneity in the subcontinental lithospheric mantle with garnets and xenoliths: Geophysical implications: *Tectonophysics*, v. 416, p. 289-309.

O'Reilly, S.Y., and Griffin, W.L., 2010. The continental lithosphere–asthenosphere boundary: Can we sample it?: *Lithos*, doi:10.1016/j.lithos.2010.03.016

O'Reilly, S.Y., Griffin, W.L., Poudjom Djomani, Y.H., and Morgan, P., 2001, Are lithosphere forever? Tracking changes in subcontinental lithospheric mantle through time. *GSA Today*, v. 11, p. 4-10.

Pearson, N.J., Griffin, W.L., Doyle, B.J., O'Reilly, S.Y., van Achtenbergh, E., and Kivi, K., 1999, Xenoliths from kimberlite pipes of the Lac de Gras area, Slave Craton, Canada: International Kimberlite Conference, 7th, South Africa, 11-17 April 1998, Proceedings, p. 644-658.

Peltier, W.R., Forte, A.M., Mitrovica, J.X., and Dziewonski, A.M., 1992, Earth's gravitational field: Seismic tomography resolves the enigma of the Laurentian anomaly: *Geophysical Research Letters*, v. 19, p. 1555-1558.

Percival, J.A., and West, G.F., 1994, The Kapuskasing uplift: a geological and geophysical synthesis: *Canadian Journal of Earth Sciences*, v. 31, p. 1256-1286.

Petitjean, S., Rabinowicz, M. Grégoire, M., and Chevrot, S., 2006, Differences between Archean and Proterozoic lithospheres: Assessment of the possible major role of thermal conductivity: *Geochemistry Geophysics Geosystems*, v. 7, Q03021.

Polet, J., and Anderson, D.L., 1995, Depth extent of cratons as inferred from tomographic studies: *Geology*, v. 23, p. 205-208.

Promprated, P., Taylor, L., Floss, C., Malkovets, V., Anand, M., Griffin, W., Pokhilenko, N., and Sobolev, N., 2003, Diamond inclusions from Snap Lake, NWT, Canada: International Kimberlite Conference, 8th, Canada, 22-27 June 2003, Extended Abstracts.

Robertson, G.S., and Woodhouse, J.H., 1997, Comparison of P and S station corrections and their relationship to upper mantle structure: *Journal of Geophysical Research*, v. 102, p. 22,355-22,366.

Rondenay, S., Bostock, M.G., Hearn, T.M., White, D.J., Wu, H., Sénéchal, G., Ji, S., and Mareschal, M., 2000, Teleseismic studies of the lithosphere below the Abitibi-Grenville Lithoprobe transect: *Canadian Journal of Earth Sciences*, v. 37, p. 415-426.

Ross, G.M., 2002, Evolution of Precambrian continental lithosphere in Western Canada: results from Lithoprobe studies in Alberta and beyond: *Canadian Journal of Earth Sciences*, v. 39, p. 413-437.

Ross, G.M., and Eaton D.W., 2002, Proterozoic tectonic accretion and growth of western Laurentia: results from Lithoprobe studies in northern Alberta: *Canadian Journal of Earth Sciences*, v. 39, p. 313-329.

Ross, G.M., Parrish, R.R., Villeneuve, M.E., and Bowring, S.A., 1991, Geophysics and geochronology of the crystalline basement of the Alberta Basin, western Canada: *Canadian Journal of Earth Sciences*, v. 28, p. 512-522.

Sage, R.P., 1991, Alkalic rock, carbonatite and kimberlite complexes of Ontario, Superior Province: Ontario Geological Survey, *Geology of Ontario Special Volume 4, Part I*, p. 683-709.

Sage, R.P., 2000, Kimberlites of the Lake Timiskaming Structural Zone: Ontario Geological Survey Supplement, Open File Report 6018, 123 p.

Schmidberger, S.S., and Francis, D., 2001, Constraints on the Trace Element composition of the Archean mantle Root beneath Somerset Island, Arctic Canada: *Journal of Petrology*, v. 42, p. 1095-1117.

Schmidberger, S.S., Simonetti, A., and Francis, D., 2001, Sr-Nd-Pb isotope systematics of mantle xenoliths from Somerset Island kimberlites: Evidence for lithospheric stratification beneath Arctic Canada: *Geochimica et Cosmochimica Acta*, v. 65, p. 4243-4255.

Schruben, P.G., Arndt, R.E., and Bawiec, W.J., 1997, Geology of the conterminous United States at 1:2,500,000 scale: a digital representation of the 1974 P.B. King and H.M. Beikman map. U.S.: Geological Survey, Digital data series DDS-11, Release 2.

Scully, K.R., Canil, D., and Schulze, D.J., 2004, The lithospheric mantle of the Archean Superior Province as imaged by garnet xenocryst geochemistry: *Chemical Geology*, v. 207, p. 189-221

Shirey, S.B., Richardson, S.H., and Harris, J.W., 2004, Integrated models of diamond formation and craton evolution: *Lithos*, v. 77, p. 923-944.

Shragge, J., Bostock, M.G., Bank, C.G., and Ellis, R.M., 2002, Integrated teleseismic studies of the southern Alberta upper mantle: *Canadian Journal of Earth Sciences*, v. 39, p. 399-411.

Smith, D., Griffin, W.L., Ryan, C.G., and Sie, S.H., 1991, Trace-element zonation in garnets from The Thumb: heating and melt infiltration below the Colorado Plateau: *Contribution to Mineralogy and Petrology*, v. 107, p. 60-79.

Snyder D., and Bruneton, M., 2007, Seismic anisotropy of the Slave craton, NW Canada, from joint interpretation of SKS and Rayleigh waves: *Geophysical Journal International* v. 169, p. 170-188.

Snyder, D., and Grütter, H.S., 2010, Lithoprobe's impact on the Canadian diamond-exploration industry: *Canadian Journal of Earth Sciences*, v. 47, p. 783-800.

Sol, S., Thomson, C.J., Kendall, J.M., White, D., VanDecar, J.C., and Asudeh, I., 2002, Seismic tomographic images of the cratonic upper mantle beneath the Western Superior

Province of the Canadian Shield - a remnant Archean slab?: *Physics of the Earth and Planetary Interiors*, v. 134, p. 53-69.

Stachel, T., and Harris, J.W., 2008, The origin of cratonic diamonds - constraints from mineral inclusions: *Ore Geology Reviews*, v. 34, p. 5-32.

Stachel, T., Banas, A., Muehlenbachs, K., Kurszlaukis, S., and Walker, E.C., 2006, Archean diamonds from Wawa (Canada): samples from deep cratonic roots predating cratonization of the Superior Province: *Contribution to Mineralogy and Petrology*, v. 151, p. 737-750.

Taylor, W.R., Tompkins, L.A., and Haggerty, S.E., 1994, Comparative geochemistry of West African kimberlites: Evidence for a micaceous kimberlite endmember of sublithospheric origin: *Geochimica et Cosmochimica Acta*, v. 58, p. 4017-4037.

Thorkelson, D.J., Mortensen, J.K., Creaser, R.A., Davidson, G.J., and Abbott, J.G., 2001, Early Proterozoic magmatism in Yukon, Canada: constraints on the evolution of northwestern Laurentia: *Canadian Journal of Earth Sciences*, v. 38, p. 1479-1494.

Trampert, J., and Woodhouse, J.H., 1995, Global phase velocity maps of Love and Rayleigh waves between 40 and 150 seconds: *Geophysical Journal International*, v.122, p. 675-690.

Trettin, H.P., 1991, Tectonic framework; chapter 4, *in* Trettin, H.P., ed., *Geology of the Innuitian Orogen and Arctic Platform of Canada and Greenland*, *Geology of Canada: Geological Survey of Canada no 3*, p. 59-66.

Türkoğlu, E., Unsworth, M., and Pana, D., 2009, Deep electrical structure of northern Alberta (Canada): implications for the diamond exploration: *Canadian Journal of Earth Science*, v. 46, p. 139-154.

van Breemen, O., Peterson, T.D., and Sandeman, H.A., 2005, U-Pb zircon geochronology and Nd isotope geochemistry of Proterozoic granitoids in the western Churchill Province: intrusive age pattern and Archean source domains: *Canadian Journal of Earth Science*, v. 42, p. 339-377.

van der Lee, S., 2001, Deep below North America: *Science*, v. 294, p. 1297-1298.

van der Lee, S., 2002, High-resolution estimates of lithospheric thickness from Missouri to Massachusetts, USA: *Earth and Planetary Science Letters*, v. 203, p. 15-23.

van der Lee, S., and Frederiksen, A., 2005, Surface wave tomography applied to the North American upper mantle: *Seismic Earth: Array analysis of broadband seismograms*, *Geophysical Monograph series 157*, American Geophysical Union, p. 67-80.

van der Lee, S., and Nolet, G., 1997, Upper mantle S velocity structure of North America: *Journal of Geophysical Research*, v. 102, p. 22,815-22,838.

van Schmus, W.R., and Hinze, W.J., 1985, The Midcontinent Rift system: Annual Review of Earth and Planetary Science Letters, v. 13, p. 345-383.

van Schmus, W.R., Bickford, M.E., and Turek, A., 1996, Proterozoic geology of the east-central midcontinent basement: Geological Society of America, Basement and Basins of Eastern North America Special Paper 308, p. 7-32.

Wallace, M.E., and Green, D.H., 1988, An experimental determination of primary carbonatite magma composition: Nature, v. 335, p. 343-346.

Wheeler, J.O., Hoffman, P.F., Card, K.D., Davidson, A., Sanford, B.V., Okulitch, A.V., and Roest, W.R., 1996, Geological map of Canada: Geological Survey of Canada, Series Map 1860A.

White, D.J., Musacchio, G., Helmstaedt, H.H., Harrap, R.M., Thurston, P.C., van der Velden, A., and Hall, K., 2003, Images of a lower-crustal oceanic slab: Direct evidence for tectonic accretion in the Archean western Superior province: Geology, v. 31, p. 997-1000.

Woolley, A.R., and Kjarsgaard, B.A., 2008, Carbonatite occurrences of the world: map and database: Geological Survey of Canada, Open File 5796, 22 p. and related database.

Wyman, D., and Kerrich, R., 2009, Plume and arc magmatism in the Abitibi subprovince: Implications for the origin of Archean continental lithospheric mantle: *Precambrian Research*, v. 168, p. 4-22.

Yuan, H., and Romanowicz, B., 2010, Lithospheric layering in the North American craton: *Nature*, v.466, p. 1063-1069.

Figure captions

Fig. 1. Shear-wave velocity perturbation relative to PREM at a depth of 150 km with the location of exposed Archean rocks, limits of crustal Archean cratons, and sedimentary cover. Craton names: NA; North Atlantic; NI; Nain, RA; Rae, SL; Slave, HN; Hearne, WY; Wyoming, GC; Grouse Creek, MH-PR; Medicine Hat - Priest River, SP; Superior, SK; Sask. Archean terranes: HBT; Hudson Bay Terrane, NCT; North Caribou Terrane. Other abbreviations: BHT; Buffalo Head Terrane, THO; Trans-Hudson Orogen, GTF; Grenville Tectonic Front, CTF; Cordilleran Tectonic Front, HB; Hudson Bay, WCSB; Western Canadian Sedimentary Basin, CP; Central Plains, MCR; Mid-continental Rift, ML; Melville Peninsula. Symbols: red diamonds; diamondiferous kimberlites, yellow diamonds; non-diamondiferous kimberlites, gray squares; lamproites. Thick black lines are major crustal fault boundaries. Alb; Alberta, NWT; Northwest Territories, Ont; Ontario, Yuk; Yukon, Qué; Québec. Cratons and tectonic subdivisions modified from Hoffman, (1989), Ross, (2002), and Foster et al. (2006). Other geological map information from Wheeler et al. (1996) and Schruben et al. (1997).

Fig. 2. a) to f): Velocity–depth profiles beneath Archean cratons of North America. Whiskers on the box plot represent the 25th, 50th (median) and 75th percentiles and the lines outline the minimum and maximum values.

Fig. 3. Surface morphology of the average seismic Archean mantle (shaded blue gradation) at depths between 100 km and 240 km with projection of the 160-200 km depth interval (oblique pattern of white lines) and the location of diamond mines, future mines, or prefeasibility

projects (white stars). WC; West Churchill. For other abbreviations and symbols see Figure 1 and Table 2. Numbers in parentheses indicate the LAB depth estimate from xenolith barometric data (Table 2).

Fig. 4. Archean seismic mantle architecture beneath North American cratons in relation to kimberlite magma pockets inferred from xenolith data (Table 2). Spheres at depth are related to the position of the kimberlites at the earth's surface (diamond-shaped). The red and yellow spheres are for diamondiferous and non-diamondiferous (or unknown) kimberlites, respectively. Abbreviations for keels: WSP: Western Superior, ESP: Eastern Superior, ML: Melville, SL: Slave, HR: Hearne-Rae, and HB: Hudson Bay.

Fig. 5. Superior craton velocity perturbation at 100 km depth with greenstone belts, carbonatites (white squares; modified from Woolley and Kjarsgaard, 2008), diamondiferous (red diamonds) and non-diamondiferous (yellow diamonds) kimberlites. The traces of the subduction zones in the upper mantle (thick blue lines) are from Ludden and Hynes (2000) and White et al. (2003). The 6 percent shell is outlined by the line with perpendicular dashes (indicating the inward direction of the shell). Green stars are the Montereian Hills (surface expression of the Cretaceous Great Meteor Hotspot). AT; Attawapiskat, DM; Desmaraisville, HB; Hudson Bay, HBT; Hudson Bay Terrane, GTF; Grenville Tectonic Front, KF; Kapuskasing Fault, KL; Kirkland Lake, KY; Kyle, LE; Lake Ellen, MCR; Mid-continental Rift, OT; Otish, TM; Timiskaming, WA; Wawa, WM; Wemindji. Note that small geological features, such as the Kapuskasing Fault, are clearly visible in the tomographic model.

Fig. 6. Sections through the cratonic Archean seismic mantle (inset) showing the trace of the 6 percent velocity perturbation shell with the location of the kimberlite magma pockets inferred from xenolith studies (filled circle; abbreviations on Table 2) or projected onto the shell (open circle). Vertical exaggeration 4 times.

Fig. 7. Schematic model of kimberlite magma formation around > 200 km deep rigid Paleo-Mesoarchean nuclei. LAB: Lithosphere-Asthenosphere Boundary. See text for more details.

Table 1. Shear-wave Velocity Perturbation Statistics Beneath Exposed Archean Cratons¹

Craton (Abbrv)	Area (Mkm²)	Mean (%)	Median (%)	Standard deviation (%)	Range (%)	Maximum value (%) at depth
Slave (SL)	0.23	6.3	6.4	0.9	4.8	8.0 at 135 km
Superior (SP)	1.57	5.7	5.7	1.5	7.7	8.8 at 165 km
Hearne (HN)	0.21	7.0	7.2	1.2	6.4	9.2 at 145 km
Rae (RA)	0.70	6.3	6.2	1.1	6.5	9.2 at 145 km
Wyoming (WY)	0.03	1.7	1.7	1.2	6.4	4.2 at 130 km
All cratons (except WY)	2.71	6.0	6.1	1.3	8.1	9.2 at 145 km

¹ Between 70 and 200 km depth

Table 2. Lithosphere-Asthenosphere Boundary Depths Estimated from Xenoliths in Kimberlites

Name (Abbrv)	Rock type	Age (Ma)	LAB (km)	6% shell	Diff (km)	Reference source
Anuri, NW Slave (AN)	K	613	175 (202)	187	12 (-15)	Griffin et al., 2004
Attawapiskat, Central Superior (AT)	K	175-180	165 (160)	172	7 (12)	Griffin et al., 2004
Aviat, Rae (AV)	K	~600	189	211	22	Snyder and Grütter, 2010
Beaver Lake, Eastern Superior (BL)	K	551	170	151	-19	Scully et al., 2004
Buffalo Hills, central Alberta (BH)	K	87	180 (189)	185	5 (-4)	Aulbach et al., 2004
Candle Lake, Saskatchewan (CD)	K	101	176	135	-41	Snyder and Grütter, 2010
Cobalt, Southern Superior (CB)	K	139-155	160 (150)	Out	n.a.	Griffin et al., 2004
Cross Lake, SW Slave (CL)	K	435-459	190 (176)	108	-82 (-68)	Griffin et al., 2004
Cross, British Columbia (CR)	K	235	200	Out	n.a.	Canil et al., 2003
Diavik Mine, Lac de Gras (DK)	K	48-56	195 (202)	194	-1 (-8)	Griffin et al., 2004
Drybones, SW Slave (DY)	K	442	160	106	-54	Carbno and Canil, 2002
Ekati, Central Lac de Gras (EK)	K	53	200 (195)	196	-4 (1)	Menzies et al., 2004
Elliott County, Kentucky (EC)	K	89	130	Out	n.a.	Griffin et al., 2004
Estes Park, Colorado (EP)	K	386	185	Out	n.a.	Eggler et al., 1988
Fort à la Corne, Saskatchewan (FC)	K	94-101	175 (186)	117	-58 (-69)	Griffin et al., 2004
Gahcho Kué, SE Slave (GK)	K	542	220 (208)	180	-40 (-28)	Kopylova and Caro, 2004
Grass Ranch, Central Montana (GR)	L	50	170	Out	n.a.	Griffin et al., 2004
Green Mountain, Colorado (GM)	K	572	190	Out	n.a.	Eggler et al., 1988
Hardy Lake, Central Slave (HD)	K	72	173	202	29	Snyder and Grütter, 2010
Jericho, Northern Slave (JE)	K	173	193 (176)	195	2 (19)	Kopylova and Russell, 2000
Kikerk, Northern Slave (KK)	K	~170	186	185	-1	Snyder and Grütter, 2010
Kirkland Lake, South Superior (KL)	K	153-165	160 (144)	Out	n.a.	Griffin et al., 2004
Kyle, Central Superior (KY)	K	1100	160 (179)	177	17 (-2)	Griffin et al., 2004
Lake Ellen, Michigan (LE)	K	180	175	Out	n.a.	Griffin et al., 2004
Mount Horeb, Virginia (MH)	K	<460	110	Out	n.a.	Griffin et al., 2004
Misery, Central Lac de Gras (MY)	K	48 - 55	200	199	-1	Doyle et al., 2003
Nothern Slave Till samples (NS)	K	-	180	191	-11	Griffin et al., 1999
Portage, Eastern Superior (PO)	K	~600	170	163	-7	Grütter et al., 2006
Potentilla, Northern Slave (PT)	K	~170	173	186	13	Snyder and Grütter, 2010
Prairie Creek, Arkansas (PC)	L	106	170	150	-20	Griffin et al., 2004
Ranch Lake, Northern Slave (RL)	K	52.1	170	191	-21	Griffin et al., 1999
Rankin Inlet, West Churchill (RI)	K	198-234	176	161	15	Snyder and Grütter, 2010
Riley County, Kansas (RC)	K	104	145	Out	n.a.	Griffin et al., 2004
Six Pack, Wisconsin (SP)	La	<1800	175	99	-76	Griffin et al., 2004
Snape Lake, Southern Slave (SL)	K	523	225 (173)	163	-62 (10)	Promprated et al., 2003
Somerset Island, Central Arctic (SO)	K	103	140	Out	n.a.	Griffin et al., 2004
State Line, Colorado (ST)	K	614	175	Out	n.a.	Coopersmith et al., 2003
Tanoma, Pennsylvania (TA)	K	89	140	Out	n.a.	Griffin et al., 2004
Tenacity, NE Slave (TE)	K	613	>150	193	<43	Griffin et al., 2004

Thumb, Colorado Plateau (TH)	La	20-30	130	Out	n.a.	Smith et al., 1991)
Tli Kwi Cho, SE Lac de Gras (TK)	K	74	200	192	-8	Pearson et al. 1999
Torrie, NW Lac de Gras (TO)	K	90-60	180	196	16	MacKenzie and Canil, 1999
Victoria Island, SW Arctic (VI)	K	270	145 (182)	160	15 (-22)	Kolebaba et al., 2003
Wawa, SW Superior (WA)	K	1097	150 (166)	Out	n.a.	Kaminsky et al., 2002
Williams, Central Montana (WI)	K	47-52	150	Out	n.a.	Carlson et al., 1999b

Notes: Rock type abbreviations: K; kimberlite, L; Lamproite; La; Lamprophyre, LAB; Lithosphere-Asthenosphere Boundary depth defined by xenolith thermobarometric studies with reference; alternative depth estimates from Snyder and Grütter (2010) are indicated in parenthesis for comparison, 6 percent shell; depth in km of the 6 percent velocity perturbation shell referring to the average seismic Archean mantle envelope; the term “Out” indicates that the kimberlite is not located over the 6 percent shell, Diff: Difference between the depths of the LAB defined by xenoliths and the 6 percent shell in km with negative sign indicating depth below the shell whereas the difference in parenthesis results from depth estimates of Snyder and Grütter (2010). Ages are from the compilation of Faure (2010).

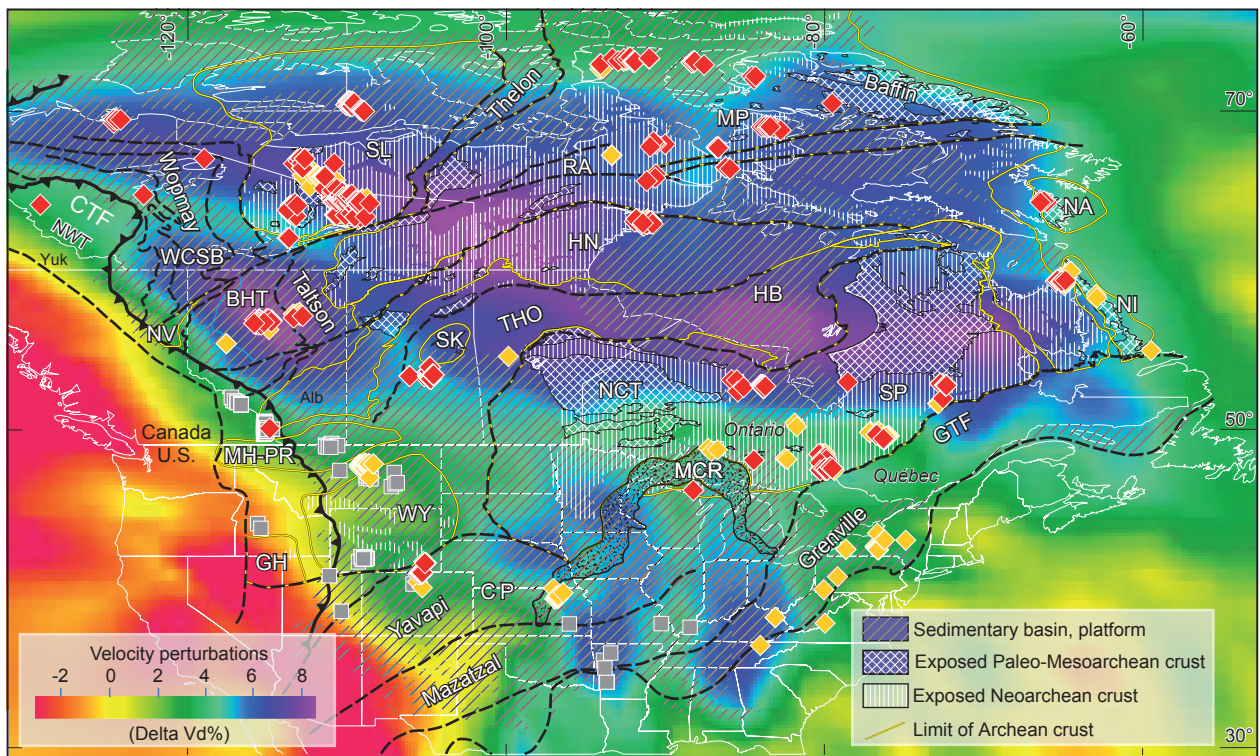


Figure 1 (Faure et al.)

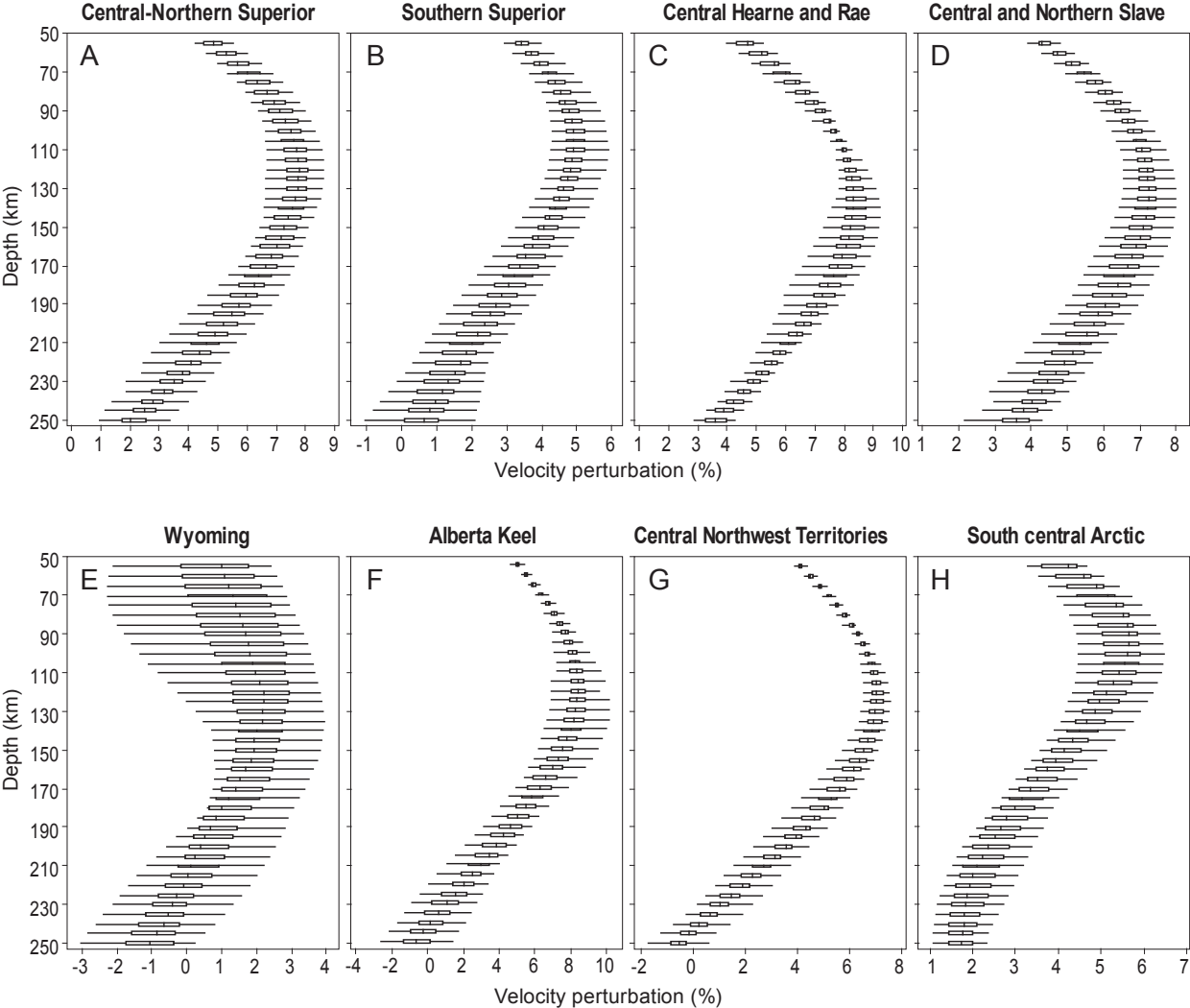


Figure 2 (Faure et al.)

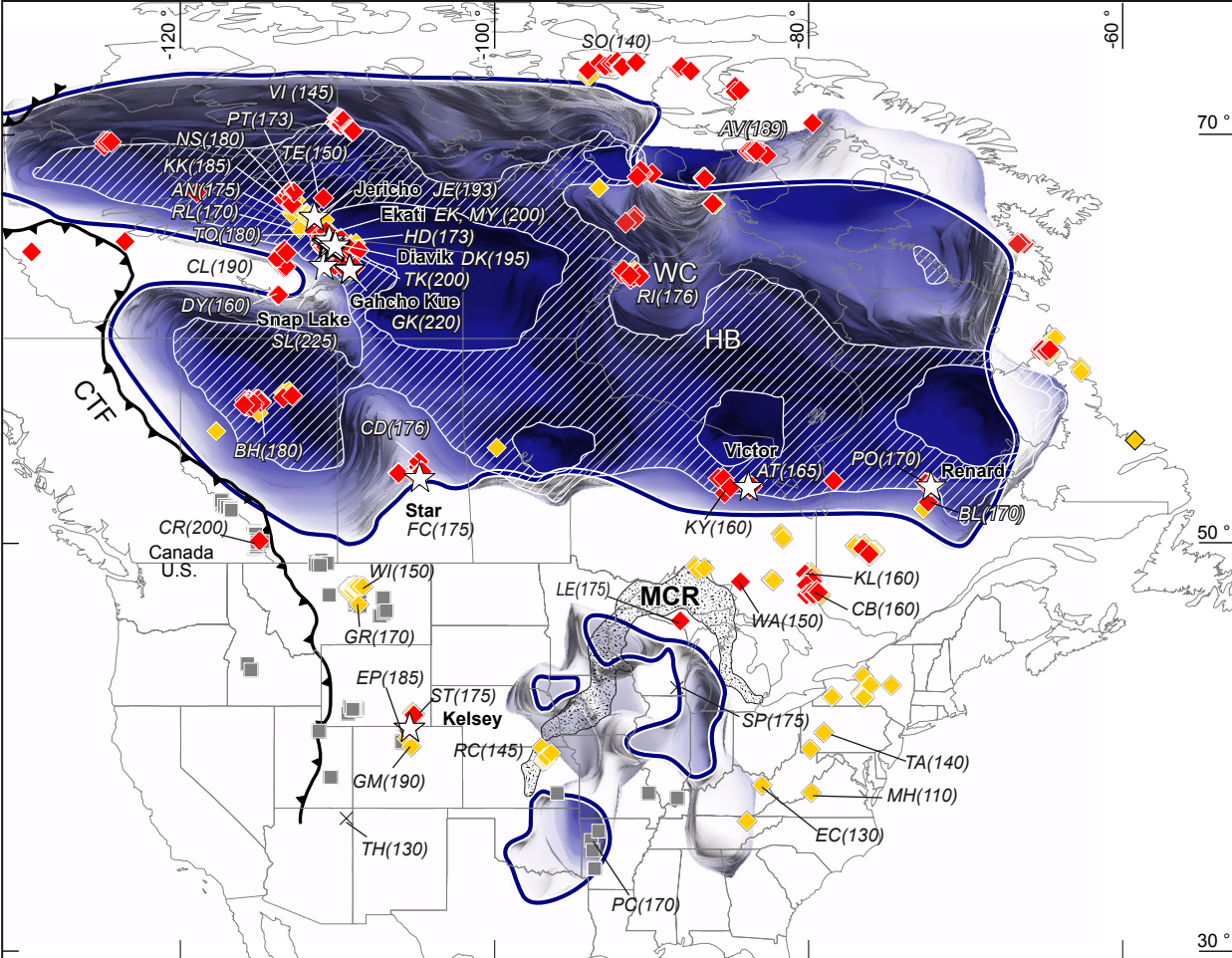


Figure 3 (Faure et al.)

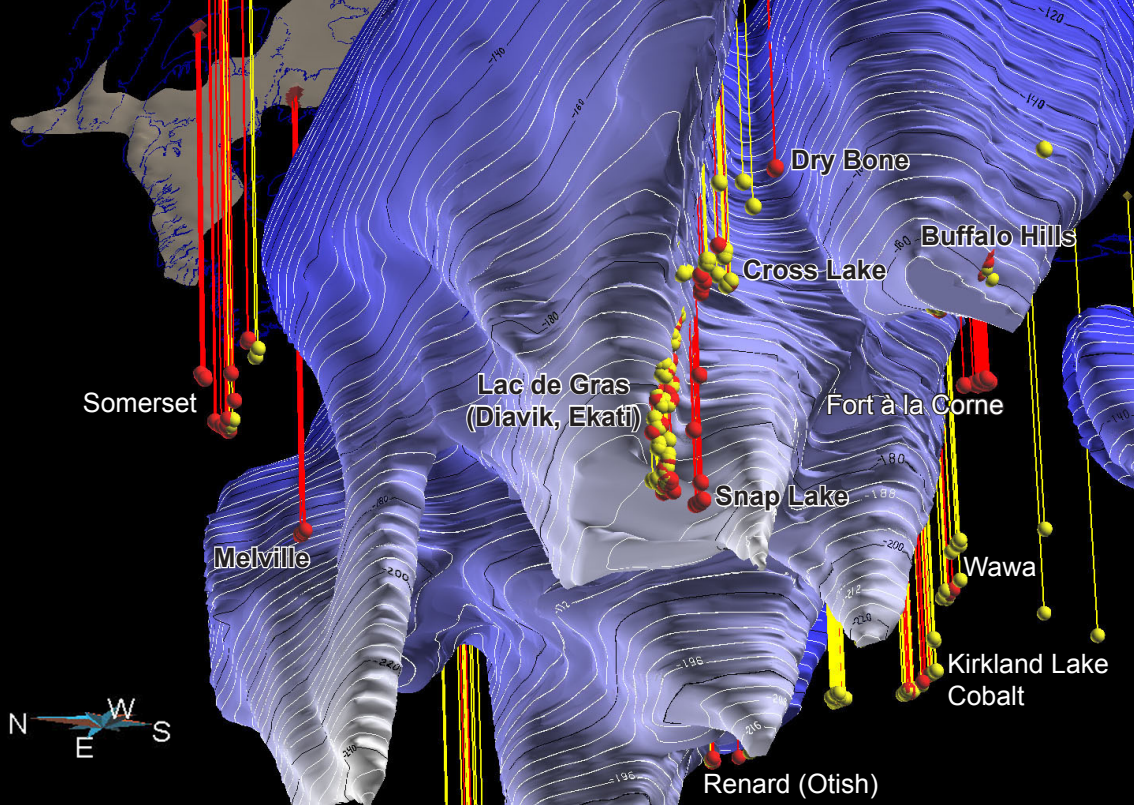


Figure 4 (Faure et al.)

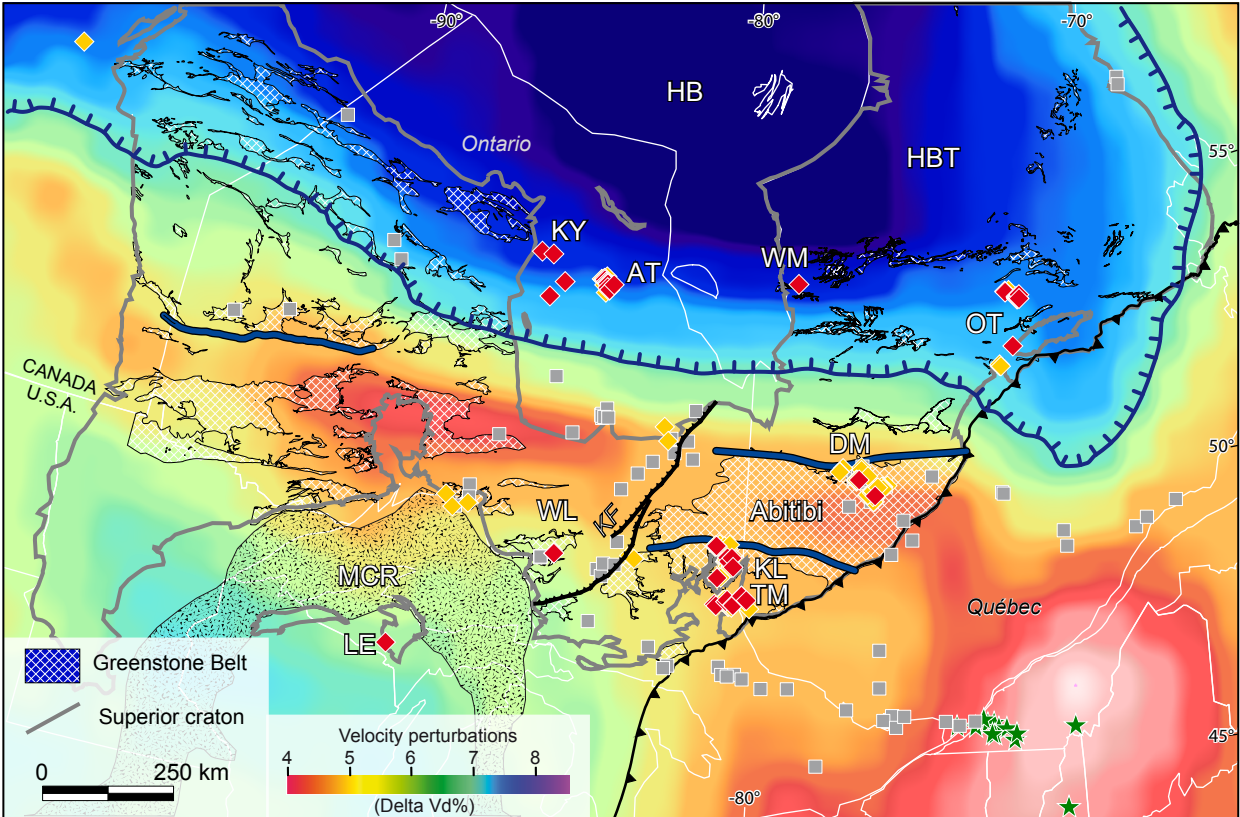


Figure 5 (Faure et al.)

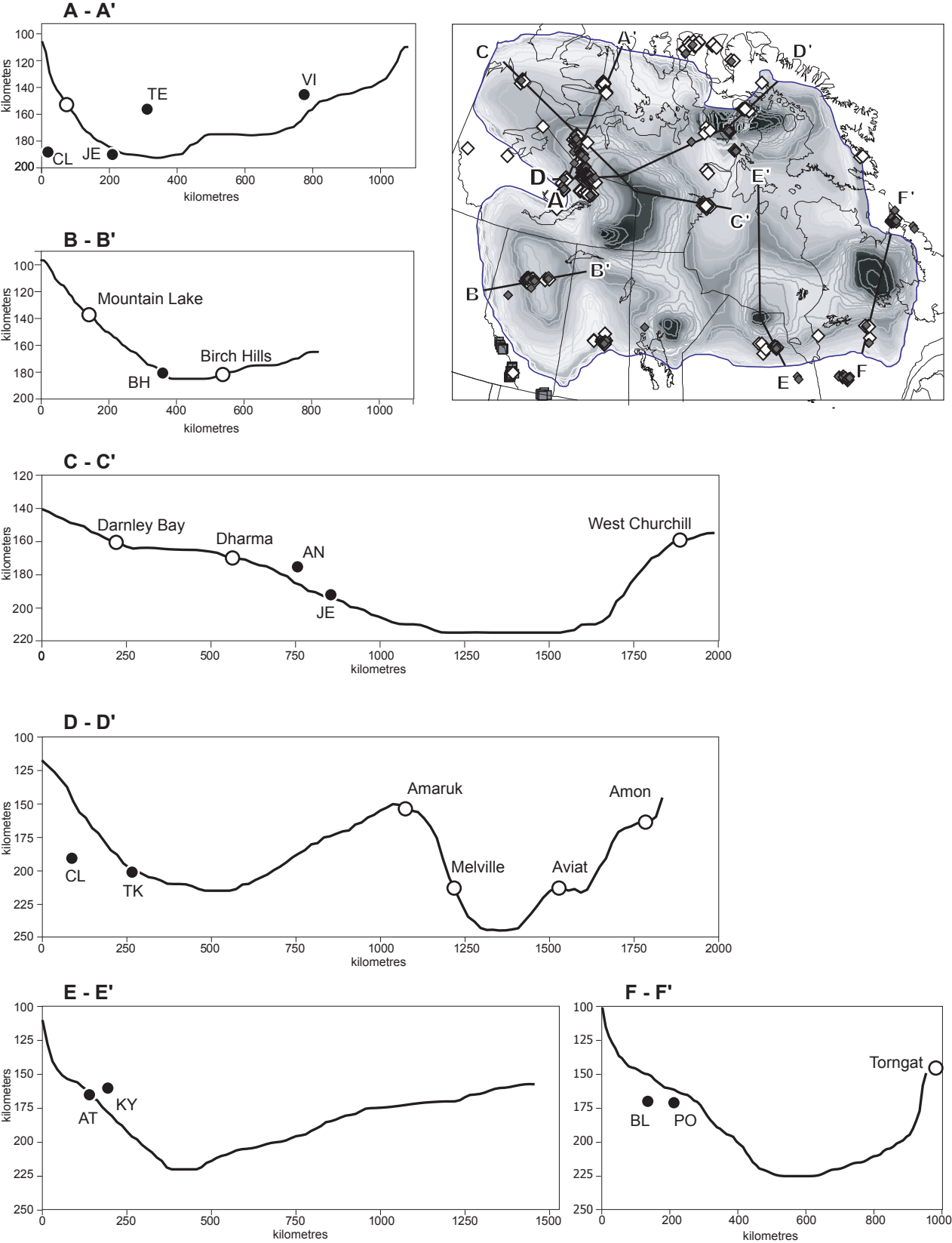


Figure 6 (Faure et al.)

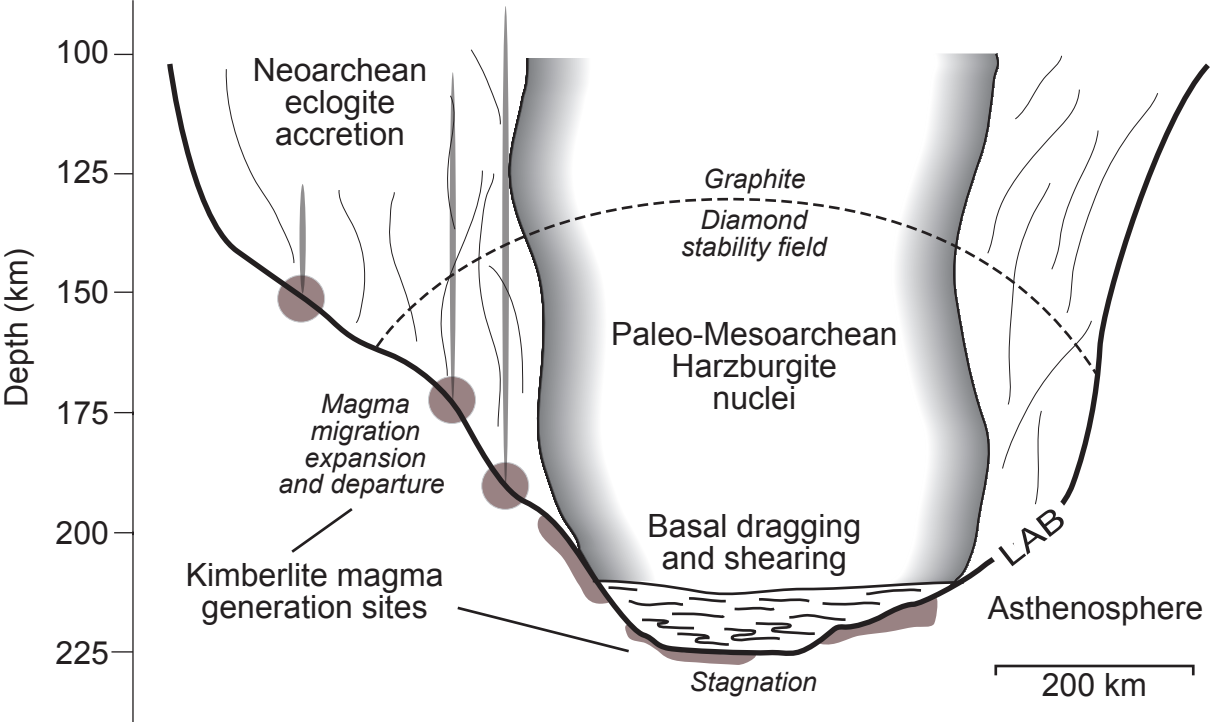


Figure 7 (Faure et al.)